

Article

Green and Facile Assembly of Diverse Fused N-Heterocycles Using Gold-Catalyzed Cascade Reactions in Water

Xiuwen Jia ¹, Pinyi Li ¹, Xiaoyan Liu ¹, Jiafu Lin ^{1,*}, Yiwen Chu ¹, Jinhai Yu ², Jiang Wang ^{3,4}, Hong Liu ^{3,4,*} and Fei Zhao ^{1,*}

- ¹ Antibiotics Research and Re-evaluation Key Laboratory of Sichuan Province, Sichuan Industrial Institute of Antibiotics, Chengdu University, Chengdu 610052, China; jiaxiuwen2018@126.com (X.J.); pinyili19950206@126.com (P.L.); 19940826097@163.com (X.L.); siiakyb@139.com (Y.C.)
- ² School of Biological Science and Technology, University of Jinan, Jinan 250022, China; bio_yujh@ujn.edu.cn
- ³ State Key Laboratory of Drug Research and CAS Key Laboratory of Receptor Research, Shanghai Institute of Materia Medical, Chinese Academy of Sciences, Shanghai 201203, China; jwang@simm.ac.cn
- ⁴ University of Chinese Academy of Sciences, Beijing 100049, China

Academic Editor: Gianfranco Favi

Received: 4 February 2019; Accepted: 4 March 2019; Published: 11 March 2019



Abstract: The present study describes an AuPPh₃Cl/AgSbF₆-catalyzed cascade reaction between amine nucleophiles and alkynoic acids in water. This process proceeds in high step economy with water as the sole coproduct, and leads to the generation of two rings, together with the formation of three new bonds in a single operation. This green cascade process exhibits valuable features such as low catalyst loading, good to excellent yields, high efficiency in bond formation, excellent selectivity, great tolerance of functional groups, and extraordinarily broad substrate scope. In addition, this is the first example of the generation of an indole/thiophene/pyrrole/pyridine/naphthalene/benzene-fused N-heterocycle library through gold catalysis in water from readily available materials. Notably, the discovery of antibacterial molecules from this library demonstrates its high quality and potential for the identification of active pharmaceutical ingredients.

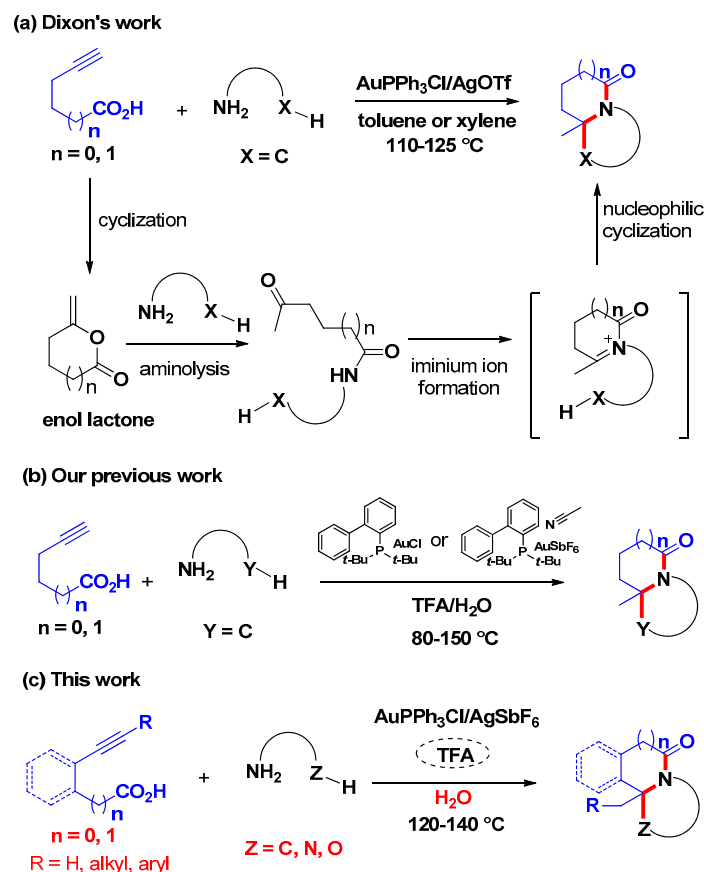
Keywords: amine nucleophiles; alkynoic acids; cascade reaction; gold catalysis; fused N-heterocycles

1. Introduction

Rapid advances in genomics and proteomics have resulted in the identification of an increasing number of novel therapeutic targets [1–5], and the existing compound libraries can no longer well meet the needs of drug screening. Therefore, it is highly demanding to develop robust synthetic methods to construct new compound libraries for drug discovery aimed at these targets [6–8]. Considering the structurally diverse targets in a wide “biological space”, high-throughput screening (HTS) of skeletally diverse compounds, which occupy a broader “chemical space”, can apparently enhance the hit rates [9,10]. In addition to skeletal diversity, drug-like properties of the compounds are equally important for the generation of high-quality compound libraries [11–14], which can increase the possibility of identifying drug-like hit compounds. As a result, privileged structures have received wide attention in drug discovery because they are widely found in natural and pharmaceutical products [15–19]. Although privileged substructure-based diversity-oriented synthesis (pDOS) provides a useful access to assemble compound libraries with high-quality [20–26], it is still challenging to develop efficient and practical approaches to generate a variety of molecular frameworks embedded with privileged structures, especially in a green and sustainable manner. With our interests to develop green and efficient protocols to synthesize valuable N-heterocycles [27–31], we herein construct a library of privileged substructure-based N-heterocycles with diverse scaffolds using gold-catalyzed

cascade reactions in water. To the best of our knowledge, this is the first example of the generation of pDOS compound library encompassing skeletal diversity, molecular complexity, and drug-like properties through gold catalysis in water.

Alkynoic acids are extensively used to react with amine nucleophiles to furnish heterocyclic compounds because of the efficient cascade reaction developed by Dixon's group [32], in which, an activated cyclic enol lactone species, which derives from alkynoic acids, is involved as the key intermediate (Scheme 1a). Dixon and co-workers disclosed linear aliphatic terminal alkynoic acids reacted smoothly with amine nucleophiles bearing a nucleophilic carbon atom in toluene or xylene to produce pyrrole- or indole-based heterocyclic frameworks catalyzed by AuPPh₃Cl/AgOTf. It should be noted that, based on Dixon's pioneering work, the reactions of alkynoic acids with amine nucleophiles in aprotic solvents such as toluene, xylene, 1,2-dichloroethane, dichloromethane, etc., have been well studied by Patil's group as well as our group [33–43]. However, the reactivity of alkynoic acids and amine nucleophiles in the environmentally friendly, abundant, and cheap solvent—water—was seldom explored [44,45], mainly because the ring opening reaction of the activated enol lactone intermediate in water at elevated temperature may lead to the failure of the cascade reaction. This reason prevented researchers' steps from investigating the nature of the cascade reaction in water. To date, only two successful examples in water were reported by our group [44,45], although the alkynoic acids were only limited to linear aliphatic terminal alkynoic acids, amine nucleophiles were only limited to amine nucleophiles carrying a nucleophilic carbon atom, and complicated Au catalysts were required (Scheme 1b). However, considering water often displays unique reactivity and selectivity which can't be obtained in common organic solvents [46–51] and it is an environmentally benign solvent, we aim to develop a more general cascade process between various alkynoic acids and amine nucleophiles in water with great interest. Despite the possibility of hydrolysis of enol lactone intermediate in water at high temperature which may result in the failure of the cascade reaction, we hypothesize that a more general cascade process could also be achieved in water but with a proper catalytic system. In the present study, we develop a greener, and more general and efficient catalytic system (AuPPh₃Cl/AgSbF₆/CF₃CO₂H) in water, which tolerates a broader substrate scope of alkynoic acids as well as amine nucleophiles. As shown in Scheme 1c, not only linear aliphatic terminal and internal alkynoic acids but also cyclic aromatic terminal and internal alkynoic acids are well tolerated. In addition, extraordinarily broad amine nucleophiles bearing a nucleophilic carbon/nitrogen/oxygen atom turned out to be suitable substrates. Besides, the reaction mechanism in water was carefully checked and studied for the first time. Interestingly, when D₂O was used as the reaction solvent, we observed the highly deuterated products generated from the H–D exchange between the reaction substrates/intermediates and D₂O. Herein, we also present the library construction of skeletally diverse *N*-heterocycles embedded with privileged structures employing different alkynoic acids and various amine nucleophiles as the building blocks. To our delight, five antimicrobial compounds were identified from this library after biological evaluation. The production of *N*-heterocycles with diverse scaffolds and the discovery of active pharmaceutical ingredients (APIs) demonstrate the power of this method in both organic synthesis and medicinal chemistry.



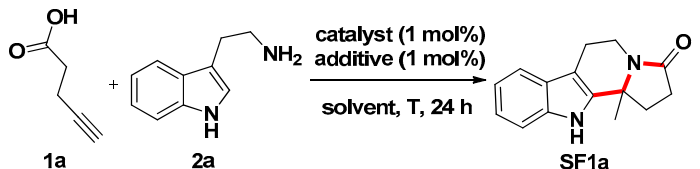
Scheme 1. Gold-catalyzed tandem reactions between alkynoic acids and amine nucleophiles. (a). Dixon's work. (b). Our previous work. (c). This work.

2. Results and Discussion

4-pentynoic acid (**1a**) and tryptamine (**2a**) were employed as the model substrates to optimize the cascade reaction conditions (Table 1). Pleasingly, treatment of starting materials **1a** and **2a** in water without any catalyst at 100 °C for 24 h gave the desired product **SF1a**, albeit with a low yield (entry 1). Then various metal catalysts were screened to improve the reaction yield. A screening of Pd, Cu, Ni, and Mn complexes (entries 2–11), disclosed, at first, that Pd(II) sources, such as PdCl₂(CH₃CN)₂ and Pd(PPh₃)₂Cl₂, NiOAc and Mn(OAc)₂, had little enhancement on the yield; while Pd(0) sources such as Pd(PPh₃)₄ and Pd₂(dba)₃; copper catalysts, such as Cu(OAc)₂ and Cu(OH)₂, and CuCl; and Ni(PPh₃)₂Cl inhibited this transformation. A subsequent survey of Ag, Ru, and Co catalysts (entries 12–16) revealed that Ag₂CO₃, AgOAc, [RuCl₂(*p*-cym)]₂, CoCl₂, and Co(acac)₂ could obviously increase the yield, affording the product **SF1a** in moderate yields (38–57%). Notably, a good yield (70%) was achieved with AuPPh₃Cl (entry 17), and increasing the temperature to 120 °C was much more efficient in improving the yield as compared with extending the reaction time to 48 h (entries 18 and 19). Encouraged by this result, an investigation of other Au catalysts at 120 °C was carried out (entries 20–24). Among them, none displayed higher catalytic reactivity than AuPPh₃Cl. To further improve the yield of the product, a series of silver salts, which were proved to be able to increase the catalytic reactivity of gold catalysts [52–57], were screened as the additives (entries 25–28). To our delight, AgSbF₆ was found to be the best choice, with which product **SF1a** was obtained in 91% yield (entry 28). In addition, other typical organic solvents were also tested as the reaction solvents, and toluene, xylene, and DCE also turned out to be suitable solvents, in which similar high isolated yields were observed (See Supplementary Materials for details). However, considering water is more environmentally benign, we then decided to use water as the solvent to explore the substrate scope of this method.

In this way, the optimal reaction conditions were identified using a catalytic system consisting of AuPPh₃Cl/AgSbF₆ in water at 120 °C for 24 h.

Table 1. Reaction condition optimization for the tandem synthesis of compound SF1a ^a.



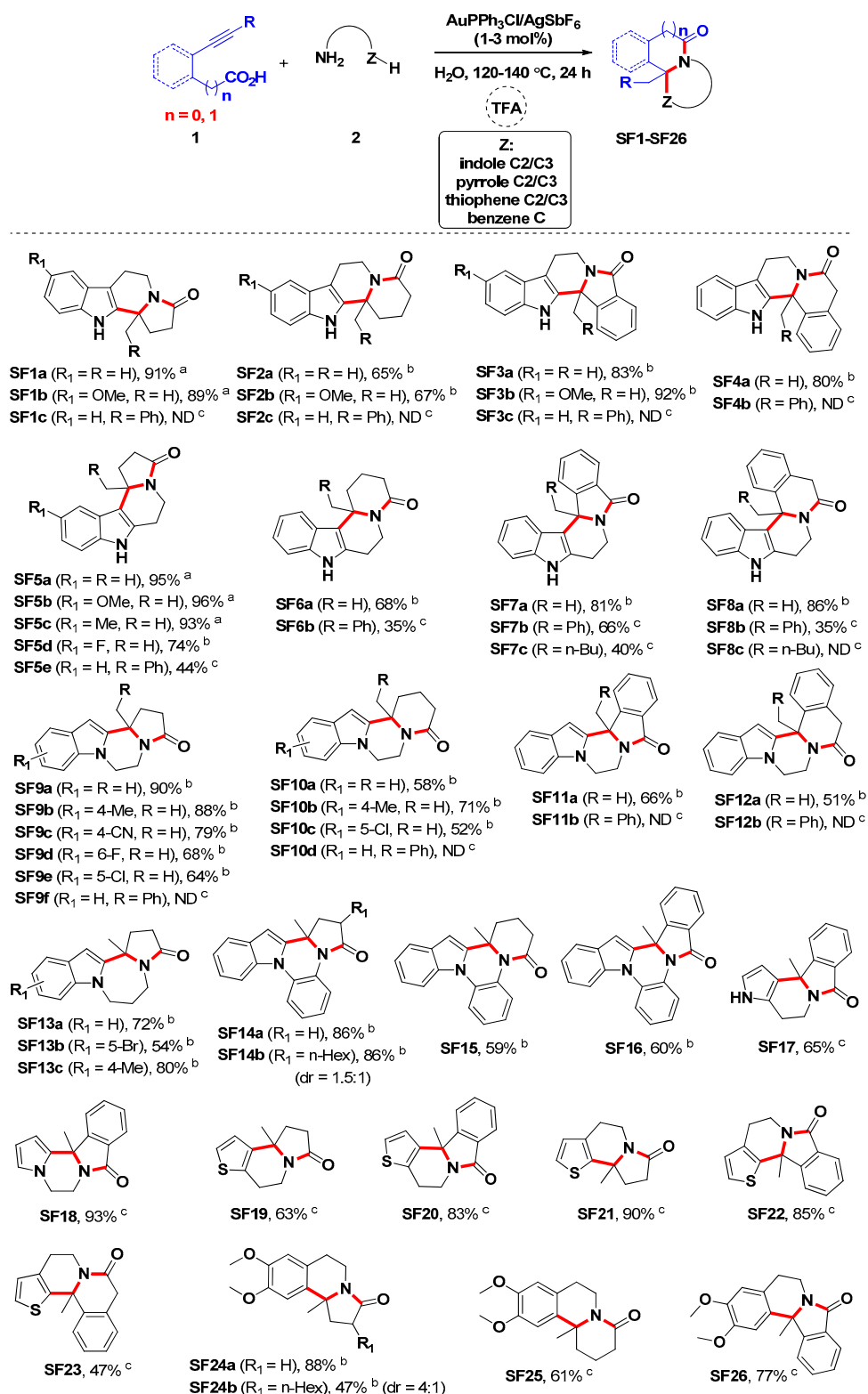
Entry	Catalyst/Additive	Solvent	T (°C)	Yield (%) ^b
1	-	H ₂ O	100	17
2	PdCl ₂ (CH ₃ CN) ₂	H ₂ O	100	26
3	Pd(PPh ₃) ₂ Cl ₂	H ₂ O	100	31
4	Pd(PPh ₃) ₄	H ₂ O	100	0
5	Pd ₂ (dba) ₃	H ₂ O	100	0
6	Cu(OAc) ₂	H ₂ O	100	trace
7	Cu(OH) ₂	H ₂ O	100	5
8	CuCl	H ₂ O	100	trace
9	NiOAc	H ₂ O	100	33
10	Ni(PPh ₃) ₂ Cl	H ₂ O	100	11
11	Mn(OAc) ₂	H ₂ O	100	25
12	Ag ₂ CO ₃	H ₂ O	100	51
13	AgOAc	H ₂ O	100	57
14	[RuCl ₂ (<i>p</i> -cym)] ₂	H ₂ O	100	48
15	CoCl ₂	H ₂ O	100	38
16	Co(acac) ₂	H ₂ O	100	50
17	AuPPh ₃ Cl	H ₂ O	100	70
18 ^c	AuPPh ₃ Cl	H ₂ O	100	76
19	AuPPh ₃ Cl	H ₂ O	120	83
20	AuBr ₃	H ₂ O	120	52
21	AuI	H ₂ O	120	46
22	Au ¹ catalyst ^d	H ₂ O	120	81
23	Au ² catalyst ^e	H ₂ O	120	78
24	Au ³ catalyst ^f	H ₂ O	120	80
25	AuPPh ₃ Cl/Ag ₂ CO ₃	H ₂ O	120	85
26	AuPPh ₃ Cl/AgOAc	H ₂ O	120	86
27	AuPPh ₃ Cl/AgOTf	H ₂ O	120	89
28	AuPPh ₃ Cl/AgSbF ₆	H ₂ O	120	91

^a Reaction conditions: 4-pentynoic acid **1a** (0.6 mmol), tryptamine **2a** (0.5 mmol), catalyst/additive (0.005 mmol), and solvent (4.0 mL). ^b Yield refers to isolated yield. ^c The reaction was performed for 48 h. ^d Au¹ catalyst = Chloro[(1,1'-biphenyl-2-yl)di-*tert*-butylphosphine]gold(I). ^e Au² catalyst = Chloro[1,3-bis(2,6-diisopropylphenyl)imidazol-2-ylidene]gold(I). ^f Au³ catalyst = (Acetonitrile)[(2-biphenyl)di-*tert*-butylphosphine]gold(I) hexafluoroantimonate.

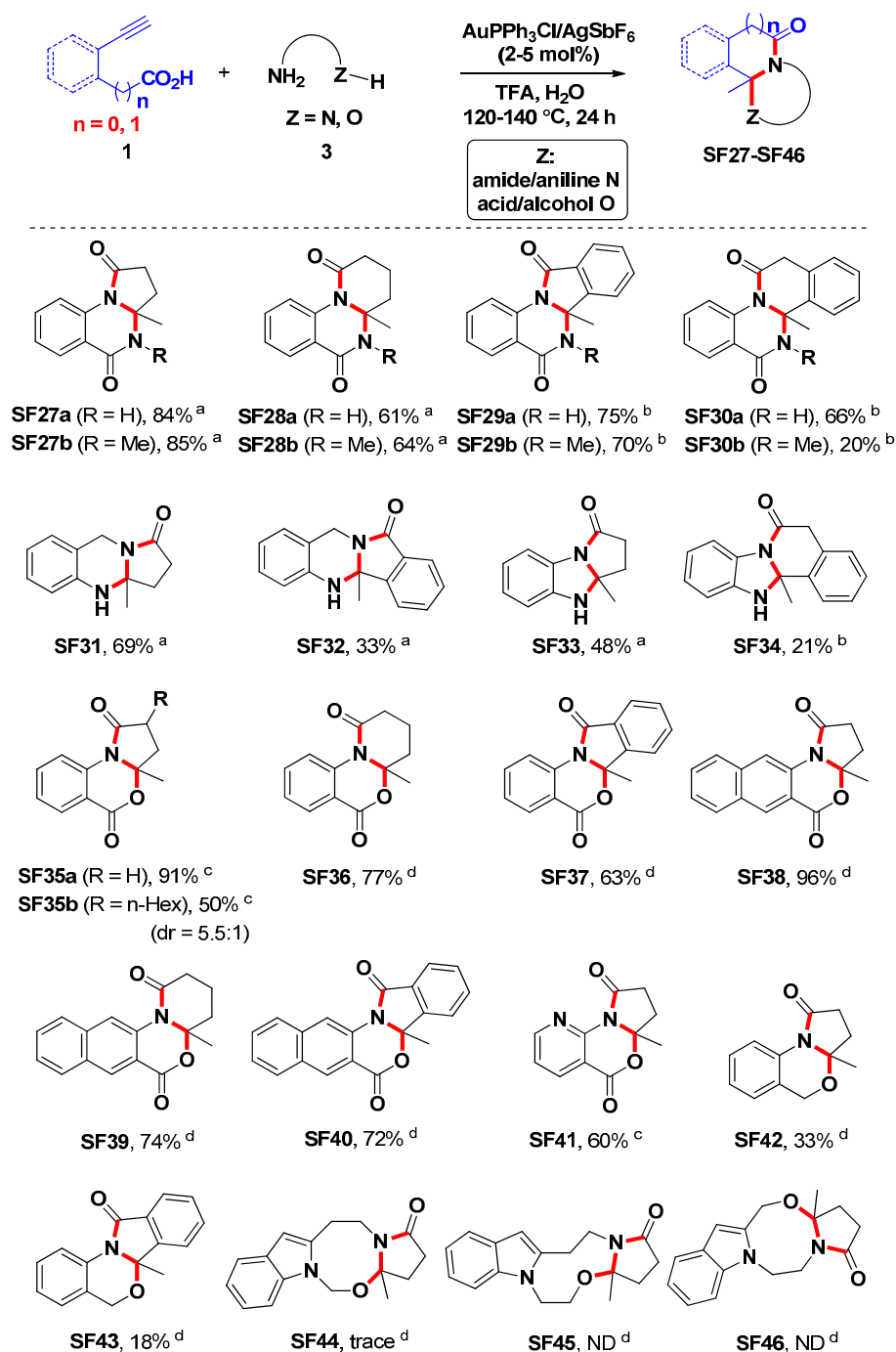
After determining the optimal reaction conditions, we then began to construct a high-quality library of privileged substructure-based *N*-heterocycles with diverse scaffolds. We first examined the generality of the process with various amine nucleophiles **2** containing a nucleophilic carbon on a heteroaromatic or aromatic ring. In general, this process tolerated a variety of amine nucleophiles **2** and alkyne acids **1**, and 26 scaffolds embedded with privileged structures were furnished in good to high yields in water under optimal or modified reaction conditions (Scheme 2). For example, tryptamines reacted smoothly with terminal alkyne acids such as 4-pentynoic acid under standard conditions to give products SF1a and SF1b in high yields. The reactions of tryptamines with other terminal alkyne acids, such as 5-hexynoic acid, 2-ethynylbenzoic acid, and 2-(2-ethynylphenyl)acetic acid, also afforded the corresponding products (SF2a, SF2b, SF3a, SF3b, and SF4a) in good to high yields under a modified two-step one-pot process, in which CF₃CO₂H (TFA) was added to promote the iminium ion formation. In addition, internal alkyne acids,

such as 5-phenylpent-4-ynoic acid, 6-phenylhex-5-ynoic acid, 2-(phenylethynyl)benzoic acid, and 2-(2-(phenylethynyl)phenyl)acetic acid, were also tested as the substrates. Unfortunately, they all failed to react with tryptamines to give the desired products (**SF1c**, **SF2c**, **SF3c**, and **SF4b**) even under further improved conditions. Interestingly, 2-(1*H*-indol-2-yl)ethylamines could undergo this transformation with terminal alkynoic acids as well as internal alkynoic acids to yield the desired products **SF5–SF8** in 35–96% yields. It should be noted that no N1 ring closure products were observed when 2-(1*H*-indol-2-yl)ethylamines were used as the amine nucleophiles, suggesting excellent selectivity of this cascade process. This may be because the C3 nucleophilicity is stronger than N1 nucleophilicity [58]. Likewise, the reactivity of 2-(1*H*-indol-1-yl)ethanamines in this cascade reaction was very similar to that of tryptamines. They reacted well with terminal alkynoic acids while their reactions with internal alkynoic acids failed to give the desired products (**SF9–SF12**). Interestingly, the protocol was also compatible with 3-(1*H*-indol-1-yl)propan-1-amines, which furnished products **SF13** carrying a seven-membered ring in 54–80% yields. Similarly, products **SF14–SF16** were obtained in 59–86% yields when 2-(1*H*-indol-1-yl)anilines and alkynoic acids were subjected to the modified conditions. Notably, the indole-containing polycyclic frameworks, represented by compounds **SF1–SF16**, are regarded as valuable N-heterocycles considering their ubiquitous presence in biologically active molecules [59–63]. Subsequently, 2-(1*H*-pyrrol-2-yl)ethanamines, 2-(1*H*-pyrrol-1-yl)ethanamines, 2-(thiophen-2-yl)ethanamines, and 2-(thiophen-3-yl)ethanamines were employed as amine nucleophiles. Their reactions with diverse alkynoic acids took place successfully to provide pyrrole- or thiophene-fused compounds **SF17–SF23** in moderate to high yields, despite the fact that stronger conditions were required. In particular, 2-phenylethanamines with electron-donating substituents on the benzene ring were also well tolerated, leading to the formation of benzene-fused heterocyclic products **SF24–SF26** in yields ranging from 47 to 88%. It is also worth noting that excellent selectivity was achieved in the reactions of 2-(1*H*-pyrrol-2-yl)ethanamine, 2-(thiophen-3-yl)ethanamine or 2-phenylethanamines, even though two potential cyclization sites existed in the final step. It should be noted that compound **SF26** is the analog of tetrahydroberberines, which were extracted from the Chinese herb *Corydalis ambigua* and exhibited a broad range of biological activities [64,65].

To further broaden the substrate scope of this approach, amine nucleophiles **3** containing a nucleophilic heteroatom ($Z =$ amide/aniline N, acid/alcohol O) were tested as substrates. Overall, this protocol was also applicable to diverse amine nucleophiles **3**, and 17 scaffolds were constructed with high efficiency (Scheme 3). For instance, the reactions of 2-aminobenzamides with various alkynoic acids worked successfully, affording benzene-fused polycyclic products **SF27–SF30** in moderate to high yields. Gratifyingly, this approach was compatible with 2-(aminomethyl)anilines and benzene-1,2-diamines, although the desired benzene-based heterocyclic products **SF31–SF34** were obtained in lower yields. Remarkably, in the case of substrates such as 2-aminobenzamides and 2-(aminomethyl)anilines, which contain two nitrogen atoms as the nucleophiles, the nitrogen atom with stronger nucleophilicity tended to attack the enol lactone intermediate and therefore the other nitrogen atom with weaker nucleophilicity attacked the iminium ion intermediate to selectively provide the corresponding products, while not in the reverse way. Besides, 2-aminobenzoic acids, 3-amino-2-naphthoic acids, or 2-aminonicotinic acids reacted with various alkynoic acids smoothly, producing the corresponding benzene-, naphthalene-, or pyridine-fused heterocyclic products **SF35–SF41** in yields of 50–96%. Surprisingly, 2-aminobenzyl alcohols were also found to be suitable substrates, which could undergo the cascade reaction with alkynoic acids to give the desired benzene-fused polycyclic products **SF42** and **SF43**, albeit with lower yields. In addition, we also tried to synthesize the indole-fused compounds **SF44–SF46** embedded with an eight- or nine-membered ring; unfortunately, we failed. This may be attributed to the low reactivities of the amine nucleophiles and the instability of the large rings in energetics.



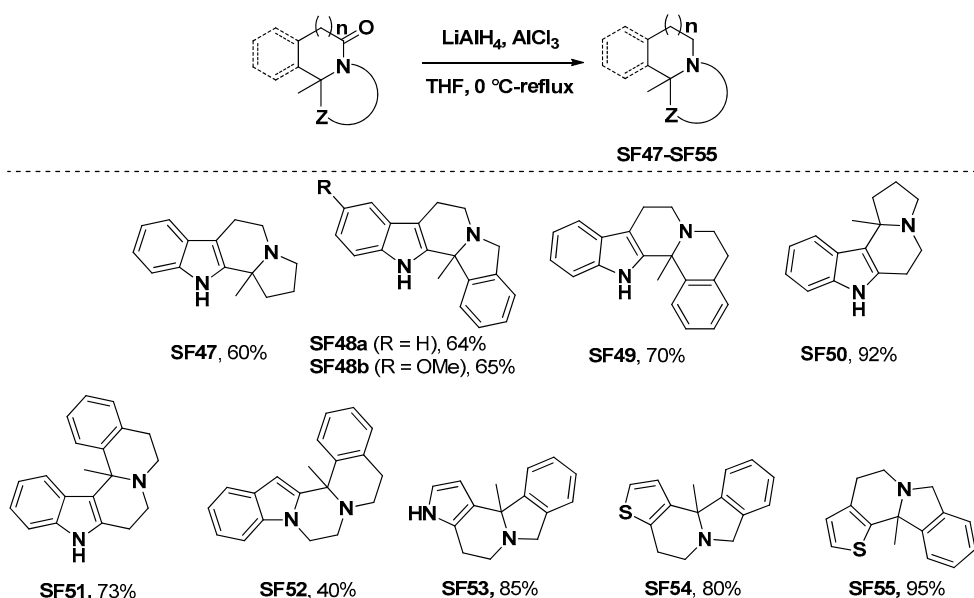
Scheme 2. Generation of scaffold diversity. ^a Reaction conditions: alkynoic acids **1** (0.6 mmol), amine nucleophiles **2** (0.5 mmol), AuPPh₃Cl/AgSbF₆ (0.005 mmol), H₂O (4.0 mL), and 120 °C, 24 h. ^b Reaction conditions: (i) alkynoic acids **1** (0.6 mmol), amine nucleophiles **2** (0.5 mmol), AuPPh₃Cl/AgSbF₆ (0.01 mmol), H₂O (4.0 mL), 120 °C, 20 h; (ii) TFA (0.5 mmol) was added, and then 120 °C, 4 h. ^c Reaction conditions: (i) alkynoic acids **1** (0.6 mmol), amine nucleophiles **2** (0.5 mmol), AuPPh₃Cl/AgSbF₆ (0.015 mmol), H₂O (4.0 mL), 140 °C, 20 h; (ii) TFA (0.5 mmol) was added, and then 140 °C, 4 h. ND = Not detected.



Scheme 3. Generation of scaffold diversity. ^a Reactions conditions: (i) Alkynoic acids **1** (0.6 mmol), amine nucleophiles **3** (0.5 mmol), AuPPh₃Cl/AgSbF₆ (0.01 mmol), H₂O (4.0 mL), 120 °C, 20 h; (ii) TFA (0.5 mmol) was added, and then 120 °C, 4 h. ^b The reaction was carried out at 140 °C. ^c The reaction was carried out with 5 mol% AuPPh₃Cl/AgSbF₆. ^d The reaction was performed with 5 mol% AuPPh₃Cl/AgSbF₆ at 140 °C. ND = Not detected.

The diversity of the library can be further expanded by the derivatization of the target compounds. We herein introduce the derivatization of the target compounds based on the simple reduction of the carbonyl group, and the selected results are shown in Scheme 4. Nine different scaffolds represented by indole-, pyrrole-, or thiophene-based polycyclic compounds **SF47–SF55** containing a tertiary amine were produced conveniently through an easy reduction of the corresponding precursors with LiAlH₄/AlCl₃. Notably, these scaffolds are very similar to those found in natural and pharmaceutical

agents [65]. We expect the screening of these compounds towards specific biological targets might lead to the identification of bioactive molecules.



Scheme 4. Derivatization of the target compounds in the library.

Thus, using various amine nucleophiles and alkynoic acids as the building blocks, a library of privileged substructure-based *N*-heterocycles with diverse scaffolds was constructed through gold catalysis in a green and efficient manner. It is worth noting this cascade process constructs three new bonds together with two rings in one chemical process, suggesting the high efficiency of this cascade reaction in synthesizing nitrogen-containing heterocyclic compounds. Regarding the large occurrence of nitrogen-containing heterocyclic compounds in APIs [66–68], the method presented in this paper is prospective since it could provide an environmentally benign and useful platform for the preparation of diverse nitrogen-containing heterocyclic compounds.

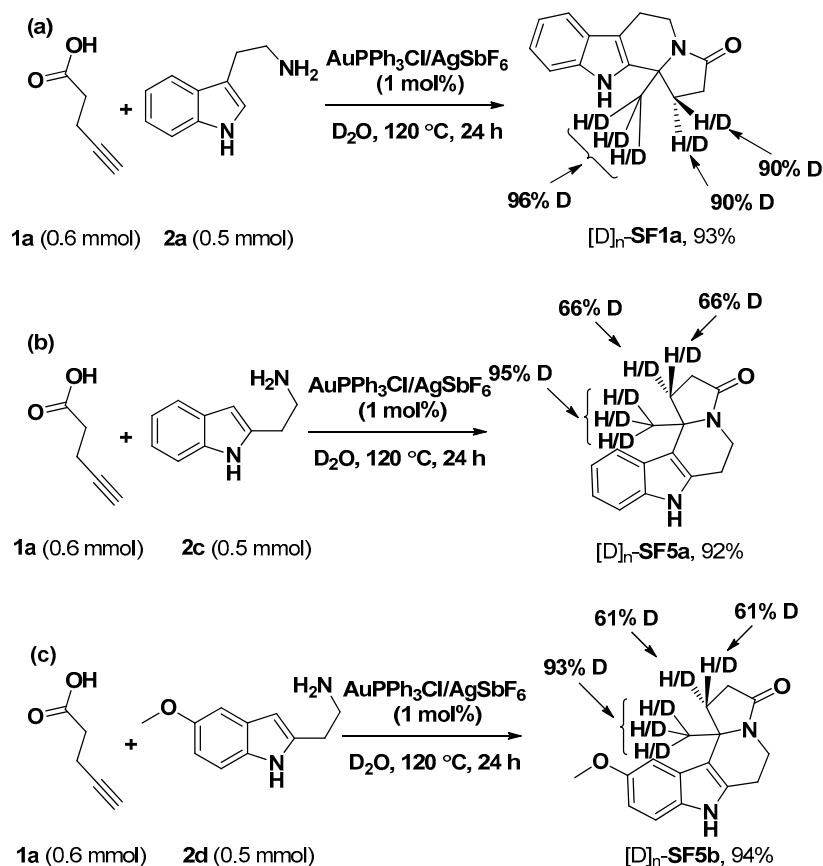
To verify our expectation that this approach could provide useful scaffolds with attractive bioactivities, a bioactivity study of this library was carried out. An initial pharmacological study of these nitrogen-containing heterocyclic compounds led to the discovery of five antimicrobial compounds—**SF9d**, **SF29b**, **SF33**, **SF36**, and **SF41**. The minimal inhibitory concentration (MIC) results revealed that compound **SF36** displayed the most potent antibacterial activity against *S. aureus* strain, with a MIC₉₀ value of 10–25 µg/mL (Table 2) (Time-kill assays and colony-forming unit studies of compounds **SF9d**, **SF29b**, **SF33**, **SF36** and **SF41** could be found in Supplementary Materials).

Table 2. MIC₉₀ of compounds **SF9d**, **SF29b**, **SF33**, **SF36**, and **SF41** against the *S. aureus* strain.

Compound	MIC ₉₀ (µg/mL)
SF9d	100–200
SF29b	50
SF33	100–200
SF36	10–25
SF41	100

Mechanistic studies were carried out with deuterium-labeling experiments, and the hydrogens of the products were assigned at first by the analysis of the ¹H-NMR, ¹³C-NMR, HSQC, HMBC, and ¹H-¹H COSY spectrum to confirm the deuterated positions (See Supplementary Materials for details). Interestingly, the reaction of 4-pentynoic acid **1a** with tryptamine **2a** in D₂O under the standard conditions afforded the deuterated product [D]_n-**SF1a**, not only at the methyl position but also at

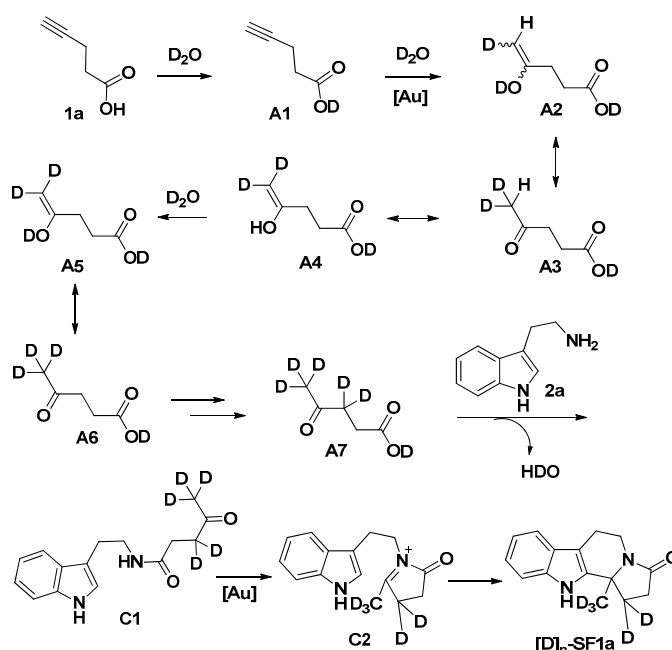
the β -position of the carbonyl (Scheme 5a). Specifically, a 96% deuteration at the methyl position and a similar deuteration (90%) of the two unequal hydrogens at the β -position of the carbonyl were observed. The reactions of 2-(1*H*-indol-2-yl)ethylamines with 4-pentynoic acid **1a** in D_2O gave the similar results (Scheme 5b,c).



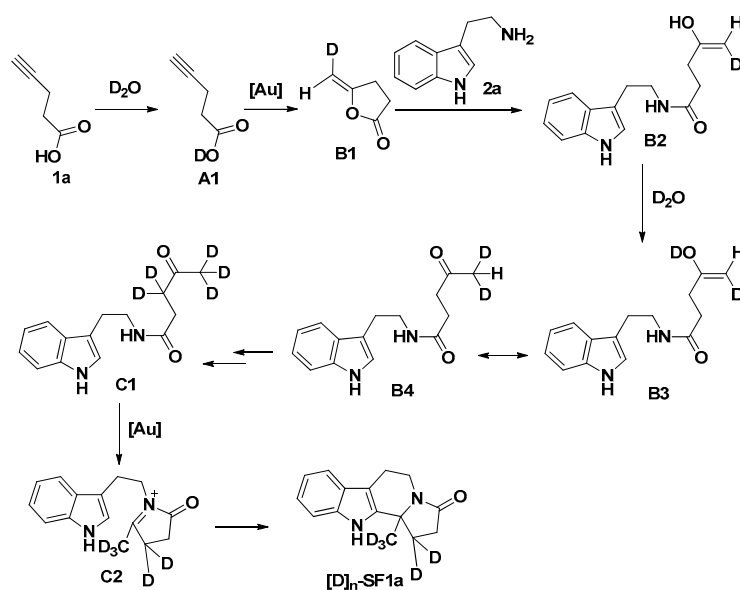
Scheme 5. Deuterium-labeling experiments.; (a) the deuterium-labeling experiment of substrates **1a** and **2a** in D_2O ; (b) the deuterium-labeling experiment of substrates **1a** and **2c** in D_2O ; (c) the deuterium-labeling experiment of substrates **1a** and **2d** in D_2O .

According to the results of deuterium-labeling experiments, we hypothesize two possible reaction pathways (Schemes 6 and 7). The reaction of with 4-pentynoic acid **1a** with tryptamine **2a** in the presence of Au catalyst in D_2O is taken as the example to illustrate the reaction pathway. The first hypothetical reaction pathway (Scheme 6) may involve the gold-catalyzed hydration of carbon–carbon triple bond, which was observed in our previous work [69]. The H–D exchange between the carboxyl group of 4-pentynoic acid **1a** and D_2O leads to the formation of intermediate **A1**. Gold-catalyzed addition of D_2O to the carbon–carbon triple bond of intermediate **A1** produces intermediate **A2**, which undergoes two keto–enol tautomerizations to give intermediate **A4**. The subsequent H–D exchange between the hydroxyl group of intermediate **A4** and D_2O affords intermediate **A5**, which undergoes keto–enol tautomerization again to give intermediate **A6**. The two acidic protons at the α -position of the carbonyl in intermediate **A6** undergo H–D exchange with D_2O via keto–enol tautomerizations to yield intermediate **A7**. The following condensation between intermediate **A7** and tryptamine **2a**, the subsequent iminium ion formation, and the final cyclization achieve the product $[D]_n\text{-SF1a}$. The second hypothetical reaction pathway is shown in Scheme 7; the H–D exchange between the carboxyl group of 4-pentynoic acid **1a** and D_2O produces intermediate **A1**. Gold-catalyzed intramolecular cyclization of intermediate **A1** produces enol lactone intermediate **B1**, which is attacked by tryptamine **2a** to give intermediate **B2**. The subsequent H–D exchange between the hydroxyl group of intermediate **B2** and D_2O yields intermediate **B3**, which undergoes enol–keto tautomerization

to provide intermediate **B4**. Similarly, the three acidic protons at the α -position of the carbonyl in intermediate **B4** undergo H–D exchange with D_2O via keto–enol tautomerizations to yield intermediate **C1**, which is converted into the product $[D]_n$ -**SF1a** via an iminium ion formation/cyclization sequence.



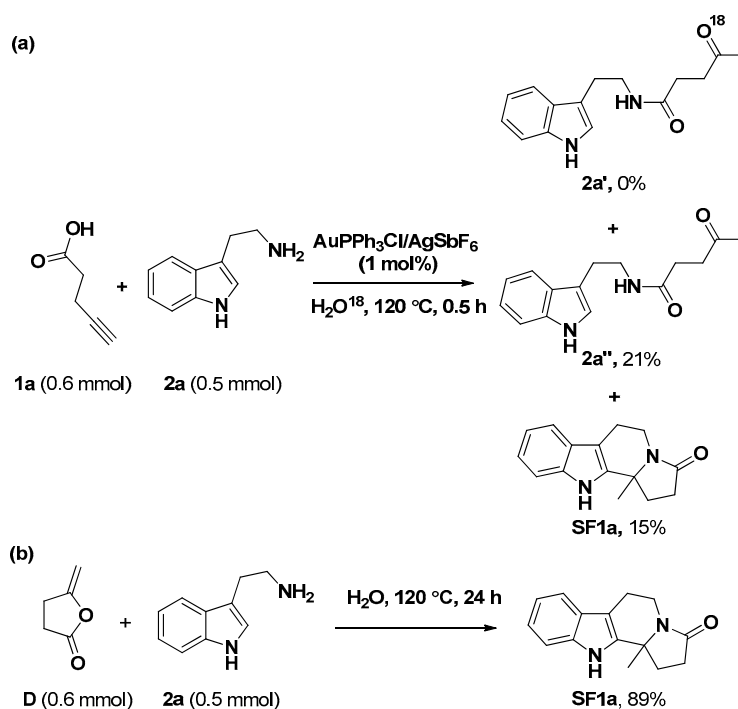
Scheme 6. Hypothetic reaction pathway 1.



Scheme 7. Hypothetic reaction pathway 2.

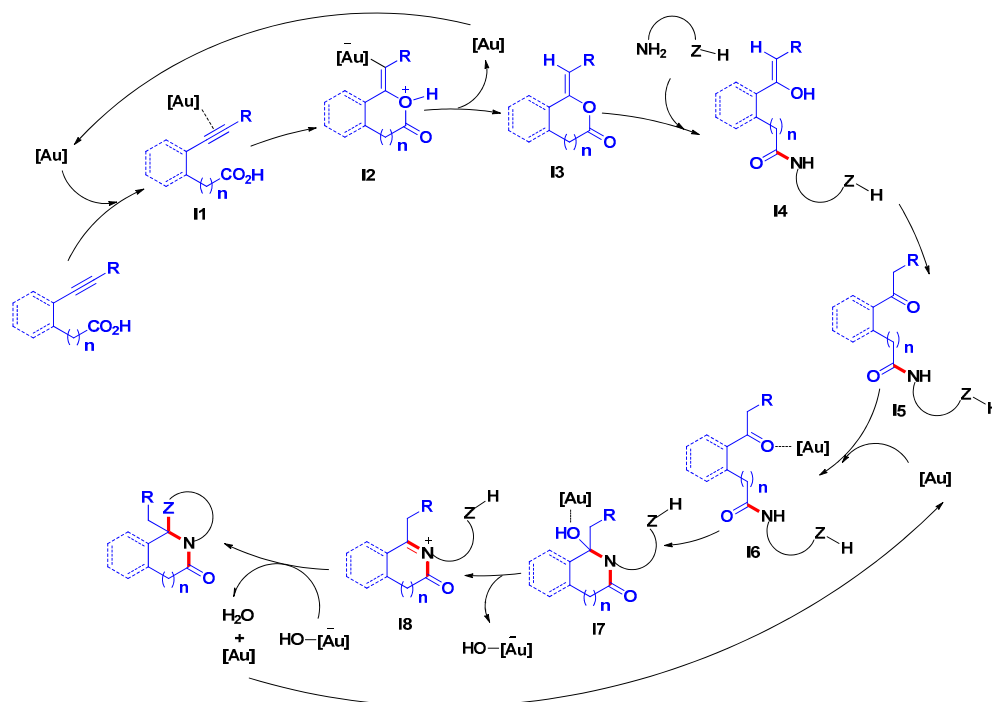
To further verify the reaction mechanism, the reaction of 4-pentynoic acid **1a** and tryptamine **2a** under gold catalysis in O^{18} -labeled water was carried out first. This reaction in H_2O^{18} was stopped after 0.5 h to track the reaction intermediates. As shown in Scheme 8a, apart from the remaining starting materials, intermediate **2a''** and the product **SF1a** were obtained in 21% and 15% yield, respectively. While the O^{18} -labeled intermediate **2a'** was not observed. This result clearly indicates the hydration of alkyne moiety, which is proposed in Scheme 6, is not involved. By contrast, the commercially purchased enol lactone **D** reacted smoothly with tryptamine **2a** without the gold catalyst (Scheme 8b).

This result shows that the enol lactone species **B1**, which is proposed in Scheme 7, is likely to be the key intermediate.



Scheme 8. Mechanistic study experiments. (a) the mechanistic experiment of substrates **1a** and **2a** in H_2O^{18} ; (b) the mechanistic experiment of substrates **D** and **2a** without catalyst/additive.

On the basis of the above results of mechanistic experiments, a final proposed reaction mechanism is outlined in Scheme 9. The proposed mechanism commences with the coordination of the gold catalyst to the carbon–carbon triple bond of alkynoic acids to produce intermediate **I1**. The subsequent intramolecular *exo* cyclization of **I1** yields intermediate **I2**. The following protodemetalation of intermediate **I2** takes place to produce the enol lactone species **I3** with the regeneration of the catalyst. Then intermediate **I3** undergoes aminolysis by amine nucleophiles to give intermediate **I4**, which tautomerizes to produce intermediate **I5**. Intermediate **I5** is converted into the iminium ion **I8** under the catalysis of the gold catalyst. The final nucleophilic cyclization of intermediate **I8** affords the desired products with the release of the gold catalyst. The stronger nucleophilicity of amine nucleophiles compared to that of H_2O results in the aminolysis of enol lactone **I3** by amine nucleophiles instead of hydrolysis by H_2O . It should be noted that the reaction solvent H_2O participates in this cascade reaction via the H–H exchange with the carboxyl group of alkynoic acids, the hydroxyl group of intermediate **I4**, and the α hydrogen atoms of the carbonyl group of intermediate **I5**, as demonstrated by deuterium-labeling experiments. Besides, TFA could promote this reaction by accelerating the formation of iminium ion **I8**.



Scheme 9. A final proposed reaction mechanism.

3. Materials and Methods

3.1. General Information

If not otherwise specified, the starting materials were obtained from commercial sources and used directly without purification. Analytical thin-layer chromatography (TLC): HSGF 254 (0.15–0.2 mm thickness). Detection under UV light at 254 nm. Column chromatography: Separations were carried out on silica gel FCP 200–300. Yields refer to isolated compounds. Melting point apparatus: a micro melting point apparatus, values are uncorrected. Nuclear magnetic resonance (NMR) apparatus: a Bruker instrument. Chemical shifts (δ) are given in ppm. Proton coupling patterns were recorded as singlet (s), doublet (d), triplet (t), quartet (q), and multiplet (m). LRMS (low-resolution mass) and HRMS (high-resolution mass) were measured on a spectrometer with an electrospray ionization (ESI) source.

3.2. General Procedure for the Preparation of Compounds SF1a, SF1b, SF5a, SF5b, and SF5c

A suspension of alkyne acids **1** (0.6 mmol), amine nucleophiles **2** (0.5 mmol), and AuPPh₃Cl/AgSbF₆ (0.005 mmol) in H₂O (4.0 mL) was stirred at 120 °C for 24 h. At ambient temperature, saturated Na₂CO₃ solution (25.0 mL) was added to the reaction mixture. The resulting mixture was then extracted with ethyl acetate (3 × 15 mL). The combined organic layers were washed with brine, and dried over Na₂SO₄. After filtration and removal of the solvents in vacuo, the crude product was purified by flash chromatography on silica gel to provide the desired product.

11b-Methyl-5,6,11,11b-tetrahydro-1H-indolizino[8,7-b]indol-3(2H)-one (SF1a): white solid (109.7 mg, yield 91%), mp 260–261 °C. ¹H-NMR (500 MHz, DMSO-*d*₆) δ 1.54 (s, 3H), 2.07–1.99 (m, 1H), 2.32–2.20 (m, 2H), 2.66–2.55 (m, 2H), 2.75–2.67 (m, 1H), 3.11–3.00 (m, 1H), 4.25–4.16 (m, 1H), 7.01–6.94 (m, 1H), 7.10–7.02 (m, 1H), 7.32 (d, *J* = 8.0 Hz, 1H), 7.39 (d, *J* = 7.8 Hz, 1H), 11.06 (s, 1H); ¹³C-NMR (100 MHz, DMSO-*d*₆) δ 171.9 (CO), 139.0 (C, Ar), 135.9 (C, Ar), 126.3 (C, Ar), 121.0 (CH, Ar), 118.6 (CH, Ar), 118.0 (CH, Ar), 111.1 (CH, Ar), 104.7 (C, Ar), 58.9 (C), 34.3 (CH₂), 32.6 (CH₂), 30.1 (CH₂), 25.0 (CH₃), 20.9 (CH₂); ESI-LRMS *m/z*: 241 [M + H]⁺; ESI-HRMS *m/z* calcd for M + H⁺ 241.1335, found: 241.1331. The characterization data is in accordance with that reported in [32].

8-Methoxy-11b-methyl-5,6,11,11b-tetrahydro-1H-indolizino[8,7-b]indol-3(2H)-one (SF1b): yellow oil (120.2 mg, yield 89%). ¹H-NMR (500 MHz, DMSO-*d*₆) δ 1.53 (s, 3H), 2.07–1.97 (m, 1H), 2.31–2.20 (m, 2H), 2.64–2.52 (m, 2H), 2.73–2.64 (m, 1H), 3.10–2.98 (m, 1H), 3.74 (s, 3H), 4.24–4.15 (m, 1H), 6.70 (dd, *J* = 8.7, 2.4 Hz, 1H), 6.89 (d, *J* = 2.3 Hz, 1H), 7.20 (d, *J* = 8.7 Hz, 1H), 10.88 (s, 1H); ¹³C-NMR (125 MHz, DMSO-*d*₆) δ 171.9 (CO), 153.2 (C, Ar), 139.7 (C, Ar), 130.9 (C, Ar), 126.6 (C, Ar), 111.7 (CH, Ar), 110.8 (CH, Ar), 104.6 (C, Ar), 100.2 (CH, Ar), 58.9 (C), 55.4 (OCH₃), 34.3 (CH₂), 32.6 (CH₂), 30.1 (CH₂), 25.0 (CH₃), 21.0 (CH₂); ESI-LRMS *m/z*: 271 [M + H]⁺; ESI-HRMS *m/z* calcd for M + H⁺ 271.1441, found: 271.1437. The characterization data is in accordance with that reported in [43].

11c-Methyl-5,6,7,11c-tetrahydro-1H-indolizino[7,8-b]indol-3(2H)-one (SF5a): yellow solid (114.2 mg, yield 95%), mp 96–97 °C. ¹H-NMR (500 MHz, DMSO-*d*₆) δ 1.54 (s, 3H), 2.02–1.92 (m, 1H), 2.27–2.17 (m, 1H), 2.54–2.47 (m, 1H), 2.65–2.54 (m, 1H), 2.81–2.67 (m, 2H), 3.16–3.04 (m, 1H), 4.27–4.18 (m, 1H), 7.00–6.92 (m, 1H), 7.08–7.00 (m, 1H), 7.30 (d, *J* = 8.0 Hz, 1H), 7.47 (d, *J* = 7.8 Hz, 1H), 10.90 (s, 1H); ¹³C-NMR (100 MHz, DMSO-*d*₆) δ 171.5 (CO), 135.9 (C, Ar), 130.5 (C, Ar), 123.9 (C, Ar), 120.5 (CH, Ar), 118.6 (CH, Ar), 117.9 (CH, Ar), 115.3 (C, Ar), 111.1 (CH, Ar), 59.2 (C), 33.2 (CH₂), 33.2 (CH₂), 30.2 (CH₂), 25.0 (CH₃), 22.8 (CH₂); ESI-LRMS *m/z*: 241 [M + H]⁺; ESI-HRMS *m/z* calcd for M + H⁺ 241.1335, found: 241.1332. The characterization data is in accordance with that reported in [43].

10-Methoxy-11c-methyl-5,6,7,11c-tetrahydro-1H-indolizino[7,8-b]indol-3(2H)-one (SF5b): pale yellow solid (129.5 mg, yield 96%), mp 193–194 °C. ¹H-NMR (500 MHz, DMSO-*d*₆) δ 1.54 (s, 3H), 2.01–1.91 (m, 1H), 2.27–2.18 (m, 1H), 2.64–2.52 (m, 2H), 2.79–2.65 (m, 2H), 3.14–3.03 (m, 1H), 3.77 (s, 3H), 4.25–4.15 (m, 1H), 6.69 (dd, *J* = 8.7, 2.4 Hz, 1H), 6.93 (d, *J* = 2.3 Hz, 1H), 7.19 (d, *J* = 8.7 Hz, 1H), 10.72 (s, 1H); ¹³C-NMR (100 MHz, DMSO-*d*₆) δ 171.5 (CO), 153.1 (C, Ar), 131.3 (C, Ar), 131.0 (C, Ar), 124.2 (C, Ar), 115.1 (C, Ar), 111.7 (CH, Ar), 109.8 (CH, Ar), 100.6 (CH, Ar), 59.2 (C), 55.5 (OCH₃), 33.2 (CH₂), 33.0 (CH₂), 30.1 (CH₂), 24.8 (CH₃), 22.9 (CH₂); ESI-LRMS *m/z*: 271 [M + H]⁺; ESI-HRMS *m/z* calcd for M + H⁺ 271.1441, found: 271.1437. The characterization data is in accordance with that reported in [43].

10,11c-Dimethyl-5,6,7,11c-tetrahydro-1H-indolizino[7,8-b]indol-3(2H)-one (SF5c): pale yellow oil (118.4 mg, yield 93%). ¹H-NMR (500 MHz, DMSO-*d*₆) δ 1.53 (s, 3H), 2.02–1.91 (m, 1H), 2.29–2.17 (m, 1H), 2.38 (s, 3H), 2.50–2.46 (m, 1H), 2.64–2.54 (m, 1H), 2.80–2.65 (m, 2H), 3.15–3.03 (m, 1H), 4.26–4.15 (m, 1H), 6.86 (dd, *J* = 8.2, 1.0 Hz, 1H), 7.18 (d, *J* = 8.2 Hz, 1H), 7.25 (s, 1H), 10.75 (s, 1H); ¹³C-NMR (125 MHz, DMSO-*d*₆) δ 171.5 (CO), 134.2 (C, Ar), 130.5 (C, Ar), 127.1 (C, Ar), 124.1 (C, Ar), 122.0 (CH, Ar), 117.6 (CH, Ar), 114.8 (C, Ar), 110.8 (CH, Ar), 59.2 (C), 33.3 (CH₂), 33.2 (CH₂), 30.2 (CH₂), 25.0 (CH₃), 22.8 (CH₂), 21.3 (CH₃); ESI-LRMS *m/z*: 255 [M + H]⁺; ESI-HRMS *m/z* calcd for M + H⁺ 255.1492, found: 255.1489. The characterization data is in accordance with that reported in [43].

3.3. General Procedure for the Preparation of Compounds SF1c, SF2–SF4, SF5d, SF5e and SF6–SF46

A suspension of alkynoic acids **1** (0.6 mmol), amine nucleophiles **2** or **3** (0.5 mmol), and AuPPh₃Cl/AgSbF₆ (with the amount indicated) in H₂O (4.0 mL) was stirred at the temperature indicated for 20 h. Then the reaction mixture was cooled to room temperature, and CF₃COOH (0.5 mmol) was added, and the resulting mixture was stirred for another 4 h at the temperature indicated. At ambient temperature, saturated Na₂CO₃ solution (25.0 mL) was added to the reaction mixture. The resulting mixture was then extracted with ethyl acetate (3 × 15 mL). The combined organic layers were washed with brine, and dried over Na₂SO₄. After filtration and removal of the solvents in vacuo, the crude product was purified by flash chromatography on silica gel to yield the desired product.

12b-Methyl-1,2,3,6,7,12b-hexahydroindolo[2,3-a]quinolizin-4(12H)-one (SF2a): white solid (82.6 mg, yield 65%), mp 255–256 °C. ¹H-NMR (500 MHz, DMSO-*d*₆) δ 1.60 (s, 3H), 1.80–1.68 (m, 2H), 1.97–1.86 (m, 1H), 2.32–2.21 (m, 1H), 2.45–2.32 (m, 2H), 2.61–2.53 (m, 1H), 2.69–2.62 (m, 1H), 2.99–2.87 (m, 1H), 4.90–4.81 (m, 1H), 7.00–6.93 (m, 1H), 7.10–7.02 (m, 1H), 7.32 (d, *J* = 8.0 Hz, 1H), 7.39 (d, *J* = 7.8 Hz, 1H), 10.92 (s, 1H); ¹³C-NMR (125 MHz, DMSO-*d*₆) δ 167.9 (CO), 139.7 (C, Ar), 136.0 (C, Ar), 126.2 (C,

Ar), 120.9 (CH, Ar), 118.5 (CH, Ar), 117.9 (CH, Ar), 111.1 (CH, Ar), 105.8 (C, Ar), 56.4 (C), 35.6 (CH₂), 34.8 (CH₂), 31.8 (CH₂), 25.3 (CH₃), 21.0 (CH₂), 16.3 (CH₂); ESI-LRMS *m/z*: 255 [M + H]⁺; ESI-HRMS *m/z* calcd for M + H⁺ 255.1492, found: 255.1488. The characterization data is in accordance with that reported in [43].

9-Methoxy-12b-methyl-1,2,3,6,7,12b-hexahydroindolo[2,3-a]quinolizin-4(12H)-one (SF2b): pale yellow solid (95.4 mg, yield 67%), mp 190–191 °C. ¹H-NMR (400 MHz, DMSO-*d*₆) δ 1.59 (s, 3H), 1.79–1.66 (m, 2H), 1.97–1.84 (m, 1H), 2.42–2.21 (m, 3H), 2.66–2.51 (m, 2H), 2.99–2.86 (m, 1H), 3.74 (s, 3H), 4.90–4.79 (m, 1H), 6.70 (dd, *J* = 8.7, 2.4 Hz, 1H), 6.89 (d, *J* = 2.4 Hz, 1H), 7.20 (d, *J* = 8.7 Hz, 1H), 10.73 (s, 1H); ¹³C-NMR (125 MHz, DMSO-*d*₆) δ 167.9 (CO), 153.2 (C, Ar), 140.4 (C, Ar), 131.0 (C, Ar), 126.5 (C, Ar), 111.7 (CH, Ar), 110.7 (CH, Ar), 105.7 (C, Ar), 100.1 (CH, Ar), 56.4 (C), 55.4 (OCH₃), 35.6 (CH₂), 34.8 (CH₂), 31.8 (CH₂), 25.4 (CH₃), 21.1 (CH₂), 16.3 (CH₂); ESI-LRMS *m/z*: 285 [M + H]⁺; ESI-HRMS *m/z* calcd for M + H⁺ 285.1598, found: 285.1593. The characterization data is in accordance with that reported in [43].

13b-Methyl-7,8,13,13b-tetrahydro-5H-benzo[1,2]indolizino[8,7-b]indol-5-one (SF3a): white solid (119.4 mg, yield 83%), mp 283–284 °C. ¹H-NMR (400 MHz, DMSO-*d*₆) δ 1.86 (s, 3H), 2.75–2.63 (m, 1H), 2.85–2.75 (m, 1H), 3.47–3.36 (m, 1H), 4.59–4.47 (m, 1H), 7.03–6.93 (m, 1H), 7.15–7.05 (m, 1H), 7.44–7.34 (m, 2H), 7.58–7.49 (m, 1H), 7.79–7.68 (m, 2H), 8.32 (d, *J* = 7.9 Hz, 1H), 11.35 (s, 1H); ¹³C-NMR (100 MHz, DMSO-*d*₆) δ 167.2 (CO), 149.3 (C, Ar), 136.2 (C, Ar), 135.2 (C, Ar), 132.2 (CH, Ar), 130.3 (C, Ar), 128.6 (CH, Ar), 126.0 (C, Ar), 123.2 (CH, Ar), 122.8 (CH, Ar), 121.6 (CH, Ar), 118.9 (CH, Ar), 118.3 (CH, Ar), 111.2 (CH, Ar), 106.3 (C, Ar), 62.0 (C), 35.4 (CH₂), 25.9 (CH₃), 21.4 (CH₂); ESI-LRMS *m/z*: 289 [M + H]⁺; ESI-HRMS *m/z* calcd for M + H⁺ 289.1335, found: 289.1330. The characterization data is in accordance with that reported in [43].

10-Methoxy-13b-methyl-7,8,13,13b-tetrahydro-5H-benzo[1,2]indolizino[8,7-b]indol-5-one (SF3b): white solid (146.9 mg, yield 92%), mp 164–165 °C. ¹H-NMR (400 MHz, DMSO-*d*₆) δ 1.84 (s, 3H), 2.72–2.60 (m, 1H), 2.81–2.73 (m, 1H), 3.45–3.35 (m, 1H), 3.73 (s, 3H), 4.57–4.45 (m, 1H), 6.73 (dd, *J* = 8.7, 2.1 Hz, 1H), 6.89 (d, *J* = 2.1 Hz, 1H), 7.26 (d, *J* = 8.7 Hz, 1H), 7.58–7.47 (m, 1H), 7.77–7.67 (m, 2H), 8.29 (d, *J* = 7.9 Hz, 1H), 11.18 (s, 1H); ¹³C-NMR (125 MHz, DMSO-*d*₆) δ 167.2 (CO), 153.3 (C, Ar), 149.4 (C, Ar), 135.8 (C, Ar), 132.2 (CH, Ar), 131.2 (C, Ar), 130.2 (C, Ar), 128.6 (CH, Ar), 126.3 (C, Ar), 123.2 (CH, Ar), 122.8 (CH, Ar), 111.9 (CH, Ar), 111.5 (CH, Ar), 106.2 (C, Ar), 100.3 (CH, Ar), 62.0 (C), 55.4 (OCH₃), 35.5 (CH₂), 26.0 (CH₃), 21.5 (CH₂); ESI-LRMS *m/z*: 319 [M + H]⁺; ESI-HRMS *m/z* calcd for M + H⁺ 319.1441, found: 319.1435. The characterization data is in accordance with that reported in [43].

14b-Methyl-8,9,14,14b-tetrahydroindolo[2',3':3,4]pyrido[2,1-a]isoquinolin-6(5H)-one (SF4a): pale yellow solid (120.7 mg, yield 80%), mp 137–138 °C. ¹H-NMR (400 MHz, DMSO-*d*₆) δ 1.84 (s, 3H), 2.50–2.41 (m, 1H), 2.86–2.75 (m, 1H), 2.96–2.86 (m, 1H), 3.63 (d, *J* = 19.4 Hz, 1H), 4.08 (d, *J* = 19.2 Hz, 1H), 4.96–4.85 (m, 1H), 7.08–6.98 (m, 1H), 7.18–7.12 (m, 1H), 7.24–7.18 (m, 1H), 7.31–7.24 (m, 2H), 7.52–7.43 (m, 3H), 11.56 (s, 1H); ¹³C-NMR (100 MHz, DMSO-*d*₆) δ 169.0 (CO), 139.9 (C, Ar), 136.1 (C, Ar), 135.1 (C, Ar), 132.3 (C, Ar), 127.8 (CH, Ar), 127.5 (CH, Ar), 126.4 (CH, Ar), 126.0 (C, Ar), 124.1 (CH, Ar), 121.4 (CH, Ar), 118.8 (CH, Ar), 118.2 (CH, Ar), 111.3 (CH, Ar), 109.2 (C, Ar), 60.9 (C), 38.0 (CH₂), 37.9 (CH₂), 26.2 (CH₃), 21.0 (CH₂); ESI-LRMS *m/z*: 303 [M + H]⁺; ESI-HRMS *m/z* calcd for M + H⁺ 303.1492, found: 303.1487. The characterization data is in accordance with that reported in [43].

10-Fluoro-11c-methyl-5,6,7,11c-tetrahydro-1H-indolizino[7,8-b]indol-3(2H)-one (SF5d): pale yellow solid (95.1 mg, yield 74%), mp 104–105 °C. ¹H-NMR (400 MHz, DMSO-*d*₆) δ 1.52 (s, 3H), 1.99–1.87 (m, 1H), 2.28–2.16 (m, 1H), 2.64–2.51 (m, 2H), 2.83–2.67 (m, 2H), 3.16–3.01 (m, 1H), 4.28–4.15 (m, 1H), 6.93–6.82 (m, 1H), 7.34–7.21 (m, 2H), 11.00 (s, 1H); ¹³C-NMR (100 MHz, DMSO-*d*₆) δ 171.5 (CO), 156.7 (d, *J*_{C-F} = 231.1 Hz, CF, Ar), 132.9 (C, Ar), 132.5 (C, Ar), 124.0 (d, *J*_{C-F} = 10.1 Hz, C, Ar), 115.7 (d, *J*_{C-F} = 4.5 Hz, C, Ar), 111.9 (d, *J*_{C-F} = 9.9 Hz, CH, Ar), 108.3 (d, *J*_{C-F} = 25.8 Hz, CH, Ar), 102.9 (d, *J*_{C-F} = 23.4 Hz, CH, Ar), 59.0 (C), 33.1 (CH₂), 32.9 (CH₂), 30.1 (CH₂), 24.8 (CH₃), 22.9 (CH₂); ESI-LRMS *m/z*: 259 [M + H]⁺; ESI-HRMS *m/z* calcd for M + H⁺ 259.1241, found: 259.1238. The characterization data is in accordance with that reported in [43].

11c-Benzyl-5,6,7,11c-tetrahydro-1H-indolizino[7,8-b]indol-3(2H)-one (SF5e): pale yellow oil (69.4 mg, yield 44%). ¹H-NMR (500 MHz, CDCl₃) δ 1.78–1.65 (m, 1H), 2.22–2.09 (m, 2H), 2.72–2.60 (m, 2H), 2.97–2.85 (m, 1H), 3.08–2.98 (m, 1H), 3.21 (d, *J* = 13.9 Hz, 1H), 3.30 (d, *J* = 13.9 Hz, 1H), 4.50 (dd, *J* = 12.9, 6.4 Hz, 1H), 7.12–7.06 (m, 2H), 7.22–7.13 (m, 2H), 7.26–7.23 (m, 3H), 7.35 (d, *J* = 8.0 Hz, 1H), 7.52 (d, *J* = 7.6 Hz, 1H), 8.33 (s, 1H); ¹³C-NMR (125 MHz, CDCl₃) δ 174.3 (CO), 136.7 (C, Ar), 136.2 (C, Ar), 130.6 (C, Ar), 130.2 (2 × CH, Ar), 128.5 (2 × CH, Ar), 127.0 (CH, Ar), 124.4 (C, Ar), 121.8 (CH, Ar), 119.9 (CH, Ar), 118.5 (CH, Ar), 115.9 (C, Ar), 111.3 (CH, Ar), 63.8 (C), 44.6 (CH₂), 34.3 (CH₂), 31.6 (CH₂), 31.0 (CH₂), 23.1 (CH₂); ESI-LRMS *m/z*: 317 [M + H]⁺; ESI-HRMS *m/z* calcd for M + H⁺ 317.1648, found: 317.1651. The characterization data is in accordance with that reported in [43].

12c-Methyl-1,2,3,6,7,12c-hexahydroindolo[3,2-a]quinolizin-4(8H)-one (SF6a): white solid (86.8 mg, yield 68%), mp 132–133 °C. ¹H-NMR (400 MHz, DMSO-*d*₆) δ 1.63 (s, 3H), 1.77–1.65 (m, 2H), 2.01–1.85 (m, 1H), 2.32–2.19 (m, 1H), 2.43–2.32 (m, 1H), 2.78–2.60 (m, 3H), 3.01–2.89 (m, 1H), 4.92–4.80 (m, 1H), 6.99–6.90 (m, 1H), 7.07–6.99 (m, 1H), 7.29 (d, *J* = 8.0 Hz, 1H), 7.51 (d, *J* = 7.8 Hz, 1H), 10.91 (s, 1H); ¹³C-NMR (125 MHz, DMSO-*d*₆) δ 168.1 (CO), 136.1 (C, Ar), 131.9 (C, Ar), 124.0 (C, Ar), 120.3 (CH, Ar), 118.6 (CH, Ar), 118.5 (CH, Ar), 115.7 (C, Ar), 111.1 (CH, Ar), 57.0 (C), 35.6 (CH₂), 34.7 (CH₂), 31.9 (CH₂), 25.1 (CH₃), 23.3 (CH₂), 16.5 (CH₂); ESI-LRMS *m/z*: 255 [M + H]⁺; ESI-HRMS *m/z* calcd for M + H⁺ 255.1492, found: 255.1488. The characterization data is in accordance with that reported in [43].

12c-Benzyl-1,2,3,6,7,12c-hexahydroindolo[3,2-a]quinolizin-4(8H)-one (SF6b): pale yellow oil (57.9 mg, yield 35%). ¹H-NMR (400 MHz, DMSO-*d*₆) δ 1.52–1.41 (m, 1H), 1.68–1.54 (m, 1H), 1.90–1.78 (m, 1H), 2.24–2.05 (m, 2H), 2.61–2.53 (m, 1H), 2.81–2.64 (m, 3H), 3.24 (d, *J* = 13.6 Hz, 1H), 3.41 (d, *J* = 13.5 Hz, 1H), 4.85–4.74 (m, 1H), 6.94–6.86 (m, 1H), 7.06–6.96 (m, 3H), 7.23–7.14 (m, 3H), 7.29 (d, *J* = 8.0 Hz, 1H), 7.33 (d, *J* = 7.9 Hz, 1H), 10.95 (s, 1H); ¹³C-NMR (150 MHz, DMSO-*d*₆) δ 169.2 (CO), 137.8 (C, Ar), 136.0 (C, Ar), 133.0 (C, Ar), 130.4 (2 × CH, Ar), 127.9 (2 × CH, Ar), 126.4 (CH, Ar), 124.3 (C, Ar), 120.2 (CH, Ar), 119.0 (CH, Ar), 118.5 (CH, Ar), 114.2 (C, Ar), 111.1 (CH, Ar), 60.9 (C), 44.3 (CH₂), 35.0 (CH₂), 33.9 (CH₂), 31.7 (CH₂), 23.0 (CH₂), 16.3 (CH₂); ESI-LRMS *m/z*: 331 [M + H]⁺; ESI-HRMS *m/z* calcd for M + H⁺ 331.1805, found: 331.1812. The characterization data is in accordance with that reported in [43].

13b-Methyl-6,7-dihydro-5H-benzo[1,2]indolizino[7,8-b]indol-9(13bH)-one (SF7a): pale yellow solid (116.4 mg, yield 81%), mp 235–236 °C. ¹H-NMR (500 MHz, DMSO-*d*₆) δ 1.90 (s, 3H), 2.80–2.70 (m, 1H), 2.91–2.80 (m, 1H), 3.45–3.37 (m, 1H), 4.56–4.46 (m, 1H), 7.12–7.03 (m, 2H), 7.34–7.26 (m, 1H), 7.52–7.44 (m, 1H), 7.69–7.64 (m, 1H), 7.71 (d, *J* = 7.5 Hz, 1H), 8.12–8.03 (m, 1H), 8.27 (d, *J* = 7.8 Hz, 1H), 11.10 (s, 1H); ¹³C-NMR (125 MHz, DMSO-*d*₆) δ 167.3 (CO), 151.4 (C, Ar), 135.9 (C, Ar), 132.3 (C, Ar), 132.0 (CH, Ar), 130.2 (C, Ar), 128.1 (CH, Ar), 124.3 (C, Ar), 123.2 (CH, Ar), 123.1 (CH, Ar), 120.7 (CH, Ar), 119.0 (CH, Ar), 119.0 (CH, Ar), 111.6 (C, Ar), 111.3 (CH, Ar), 63.6 (C), 34.6 (CH₂), 25.7 (CH₃), 23.4 (CH₂); ESI-LRMS *m/z*: 289 [M + H]⁺; ESI-HRMS *m/z* calcd for M + H⁺ 289.1335, found: 289.1330. The characterization data is in accordance with that reported in [43].

13b-Benzyl-6,7-dihydro-5H-benzo[1,2]indolizino[7,8-b]indol-9(13bH)-one (SF7b): white solid (121.1 mg, yield 66%), mp 281–282 °C. ¹H-NMR (500 MHz, DMSO-*d*₆) δ 2.91–2.72 (m, 2H), 3.49–3.38 (m, 1H), 3.57 (d, *J* = 13.8 Hz, 1H), 3.85 (d, *J* = 13.9 Hz, 1H), 4.53 (dd, *J* = 13.0, 5.6 Hz, 1H), 6.95–6.87 (m, 2H), 7.08–6.98 (m, 3H), 7.20–7.08 (m, 2H), 7.39–7.30 (m, 2H), 7.46 (d, *J* = 7.4 Hz, 1H), 7.66–7.58 (m, 1H), 8.32 (d, *J* = 7.8 Hz, 1H), 8.43 (d, *J* = 7.8 Hz, 1H), 11.14 (s, 1H); ¹³C-NMR (125 MHz, DMSO-*d*₆) δ 167.7 (CO), 148.8 (C, Ar), 135.9 (C, Ar), 135.7 (C, Ar), 132.8 (C, Ar), 131.4 (CH, Ar), 131.0 (C, Ar), 130.0 (2 × CH, Ar), 127.8 (CH, Ar), 127.3 (2 × CH, Ar), 126.2 (CH, Ar), 124.4 (C, Ar), 123.9 (CH, Ar), 122.6 (CH, Ar), 120.7 (CH, Ar), 119.4 (CH, Ar), 119.1 (CH, Ar), 111.3 (CH, Ar), 111.1 (C, Ar), 67.1 (C), 42.7 (CH₂), 34.8 (CH₂), 23.4 (CH₂); ESI-LRMS *m/z*: 365 [M + H]⁺; ESI-HRMS *m/z* calcd for M + H⁺ 365.1648, found: 365.1649. The characterization data is in accordance with that reported in [43].

13b-Pentyl-6,7-dihydro-5H-benzo[1,2]indolizino[7,8-b]indol-9(13bH)-one (SF7c): pale yellow oil (68.7 mg, yield 40%). ¹H-NMR (400 MHz, CDCl₃) δ 0.77 (t, *J* = 6.7 Hz, 3H), 0.89–0.83 (m, 1H), 1.20–1.02 (m, 5H),

2.24–2.10 (m, 1H), 2.76–2.58 (m, 2H), 3.13–2.98 (m, 1H), 3.38–3.24 (m, 1H), 4.77 (dd, $J = 13.1, 6.1$ Hz, 1H), 7.23–7.12 (m, 2H), 7.31 (d, $J = 7.8$ Hz, 1H), 7.45–7.38 (m, 1H), 7.62–7.54 (m, 1H), 7.85 (d, $J = 7.5$ Hz, 1H), 7.99 (d, $J = 7.7$ Hz, 1H), 8.06 (d, $J = 7.7$ Hz, 1H), 8.23 (s, 1H); $^{13}\text{C-NMR}$ (150 MHz, CDCl_3) δ 169.4 (CO), 149.6 (C, Ar), 136.1 (C, Ar), 132.0 (CH, Ar), 131.9 (C, Ar), 131.8 (C, Ar), 128.1 (CH, Ar), 124.9 (C, Ar), 123.9 (CH, Ar), 122.9 (CH, Ar), 121.7 (CH, Ar), 120.0 (CH, Ar), 119.4 (CH, Ar), 113.5 (C, Ar), 111.4 (CH, Ar), 67.4 (C), 38.2 (CH_2), 35.3 (CH_2), 31.8 (CH_2), 24.1 (CH_2), 23.1 (CH_2), 22.5 (CH_2), 14.1 (CH_3); ESI-LRMS m/z : 345 [$\text{M} + \text{H}$] $^+$; ESI-HRMS m/z calcd for $\text{M} + \text{H}^+$ 345.1961, found: 345.1966. The characterization data is in accordance with that reported in [43].

14c-Methyl-8,9,10,14c-tetrahydroindolo[3',2':3,4]pyrido[2,1-a]isoquinolin-6(5H)-one (SF8a): yellow solid (129.8 mg, yield 86%), mp 250–251 °C. $^1\text{H-NMR}$ (400 MHz, $\text{DMSO-}d_6$) δ 1.89 (s, 3H), 2.72–2.60 (m, 1H), 2.84–2.73 (m, 1H), 3.02–2.89 (m, 1H), 3.62 (d, $J = 19.4$ Hz, 1H), 4.10 (d, $J = 19.2$ Hz, 1H), 4.95–4.86 (m, 1H), 7.15–7.04 (m, 3H), 7.30–7.19 (m, 2H), 7.44–7.38 (m, 2H), 7.59 (d, $J = 7.6$ Hz, 1H), 11.26 (s, 1H); $^{13}\text{C-NMR}$ (100 MHz, $\text{DMSO-}d_6$) δ 169.3 (CO), 141.4 (C, Ar), 136.0 (C, Ar), 134.5 (C, Ar), 132.4 (C, Ar), 127.7 (CH, Ar), 127.1 (CH, Ar), 126.2 (C, Ar), 126.1 (CH, Ar), 124.7 (CH, Ar), 120.5 (CH, Ar), 120.2 (CH, Ar), 119.2 (CH, Ar), 111.5 (CH, Ar), 111.2 (C, Ar), 61.5 (C), 38.2 (CH_2), 36.9 (CH_2), 25.7 (CH_3), 23.3 (CH_2); ESI-LRMS m/z : 303 [$\text{M} + \text{H}$] $^+$; ESI-HRMS m/z calcd for $\text{M} + \text{H}^+$ 303.1492, found: 303.1486. The characterization data is in accordance with that reported in [43].

14c-Benzyl-8,9,10,14c-tetrahydroindolo[3',2':3,4]pyrido[2,1-a]isoquinolin-6(5H)-one (SF8b): pale yellow oil (66.5 mg, yield 35%). $^1\text{H-NMR}$ (500 MHz, CDCl_3) δ 1.84–1.73 (m, 1H), 2.48–2.38 (m, 1H), 2.67–2.56 (m, 1H), 3.40 (d, $J = 13.8$ Hz, 1H), 3.96–3.76 (m, 3H), 4.79 (dd, $J = 12.7, 4.3$ Hz, 1H), 6.80–6.71 (m, 2H), 7.08–7.00 (m, 2H), 7.16–7.08 (m, 2H), 7.28–7.20 (m, 2H), 7.33–7.28 (m, 2H), 7.50–7.42 (m, 1H), 7.66 (d, $J = 7.9$ Hz, 1H), 7.96–7.88 (m, 1H), 8.36 (s, 1H); $^{13}\text{C-NMR}$ (125 MHz, CDCl_3) δ 170.6 (CO), 141.0 (C, Ar), 136.4 (C, Ar), 136.1 (C, Ar), 135.7 (C, Ar), 132.3 (C, Ar), 130.4 (2 \times CH, Ar), 128.2 (2 \times CH, Ar), 128.0 (CH, Ar), 127.7 (CH, Ar), 127.3 (C, Ar), 126.9 (CH, Ar), 126.8 (CH, Ar), 126.0 (CH, Ar), 121.6 (CH, Ar), 121.4 (CH, Ar), 120.5 (CH, Ar), 111.7 (CH, Ar), 109.9 (C, Ar), 66.5 (C), 45.0 (CH_2), 39.1 (CH_2), 38.7 (CH_2), 23.3 (CH_2); ESI-LRMS m/z : 379 [$\text{M} + \text{H}$] $^+$; ESI-HRMS m/z calcd for $\text{M} + \text{H}^+$ 379.1805, found: 379.1815. The characterization data is in accordance with that reported in [43].

12b-Methyl-1,5,6,12b-tetrahydropyrrolo[2',1':3,4]pyrazino[1,2-a]indol-3(2H)-one (SF9a): white solid (107.8 mg, yield 90%), mp 121–122 °C. $^1\text{H-NMR}$ (400 MHz, $\text{DMSO-}d_6$) δ 1.59 (s, 3H), 2.33–2.17 (m, 2H), 2.47–2.36 (m, 1H), 2.65–2.53 (m, 1H), 3.49–3.38 (m, 1H), 3.81–3.68 (m, 1H), 4.34–4.22 (m, 2H), 6.34 (s, 1H), 7.08–7.01 (m, 1H), 7.15–7.09 (m, 1H), 7.38 (d, $J = 8.1$ Hz, 1H), 7.51 (d, $J = 7.7$ Hz, 1H); $^{13}\text{C-NMR}$ (125 MHz, $\text{DMSO-}d_6$) δ 172.1 (CO), 142.1 (C, Ar), 135.2 (C, Ar), 127.6 (C, Ar), 120.7 (CH, Ar), 119.9 (CH, Ar), 119.8 (CH, Ar), 109.6 (CH, Ar), 95.5 (CH, Ar), 58.6 (C), 40.9 (CH_2), 34.3 (CH_2), 33.6 (CH_2), 29.7 (CH_2), 27.2 (CH_3); ESI-LRMS m/z : 241 [$\text{M} + \text{H}$] $^+$; ESI-HRMS m/z calcd for $\text{M} + \text{H}^+$ 241.1335, found: 241.1330. The characterization data is in accordance with that reported in [43].

11,12b-Dimethyl-1,5,6,12b-tetrahydropyrrolo[2',1':3,4]pyrazino[1,2-a]indol-3(2H)-one (SF9b): pale yellow oil (111.3 mg, yield 88%). $^1\text{H-NMR}$ (300 MHz, CDCl_3) δ 1.65 (s, 3H), 2.49–2.37 (m, 3H), 2.54 (s, 3H), 2.73–2.57 (m, 1H), 3.47–3.32 (m, 1H), 3.96–3.81 (m, 1H), 4.20 (dd, $J = 11.7, 4.7$ Hz, 1H), 4.52 (dd, $J = 13.6, 5.1$ Hz, 1H), 6.30 (s, 1H), 6.98–6.89 (m, 1H), 7.15–7.09 (m, 2H); $^{13}\text{C-NMR}$ (100 MHz, CDCl_3) δ 173.2 (CO), 141.1 (C, Ar), 135.4 (C, Ar), 130.0 (C, Ar), 127.9 (C, Ar), 121.8 (CH, Ar), 120.7 (CH, Ar), 106.8 (CH, Ar), 94.8 (CH, Ar), 59.5 (C), 41.3 (CH_2), 35.0 (CH_2), 34.3 (CH_2), 30.4 (CH_2), 27.8 (CH_3), 18.8 (CH_3); ESI-LRMS m/z : 255 [$\text{M} + \text{H}$] $^+$; ESI-HRMS m/z calcd for $\text{M} + \text{H}^+$ 255.1492, found: 255.1488. The characterization data is in accordance with that reported in [45].

12b-Methyl-3-oxo-1,2,3,5,6,12b-hexahydropyrrolo[2',1':3,4]pyrazino[1,2-a]indole-11-carbonitrile (SF9c): yellow oil (104.3 mg, yield 79%). $^1\text{H-NMR}$ (300 MHz, CDCl_3) δ 1.66 (s, 3H), 2.54–2.32 (m, 3H), 2.73–2.59 (m, 1H), 3.49–3.33 (m, 1H), 4.02–3.88 (m, 1H), 4.26 (dd, $J = 11.7, 4.8$ Hz, 1H), 4.56 (dd, $J = 13.7, 5.2$ Hz, 1H), 6.52 (s, 1H), 7.26–7.19 (m, 1H), 7.52–7.44 (m, 2H); $^{13}\text{C-NMR}$ (125 MHz, CDCl_3) δ 173.1 (CO), 144.6 (C, Ar), 135.4 (C, Ar), 129.7 (C, Ar), 125.7 (CH, Ar), 121.2 (CH, Ar), 118.7 (CN), 113.9 (CH, Ar), 102.8 (C,

Ar), 95.6 (CH, Ar), 59.3 (C), 41.5 (CH₂), 34.8 (CH₂), 33.9 (CH₂), 30.2 (CH₂), 27.6 (CH₃); ESI-LRMS *m/z*: 266 [M + H]⁺; ESI-HRMS *m/z* calcd for M + H⁺ 266.1288, found: 266.1282. The characterization data is in accordance with that reported in [45].

9-Fluoro-12b-methyl-1,5,6,12b-tetrahydropyrrolo[2',1':3,4]pyrazino[1,2-a]indol-3(2H)-one (SF9d): pale yellow solid (43.6 mg, yield 68%), mp 71–72 °C. ¹H-NMR (500 MHz, DMSO-*d*₆) δ 1.58 (s, 3H), 2.30–2.18 (m, 2H), 2.44–2.36 (m, 1H), 2.63–2.52 (m, 1H), 3.49–3.38 (m, 1H), 3.77–3.67 (m, 1H), 4.32–4.22 (m, 2H), 6.36 (s, 1H), 6.94–6.86 (m, 1H), 7.26 (dd, *J* = 10.2, 2.2 Hz, 1H), 7.50 (dd, *J* = 8.6, 5.4 Hz, 1H); ¹³C-NMR (125 MHz, DMSO-*d*₆) δ 172.1 (CO), 158.5 (d, *J*_{C-F} = 234.3 Hz, CF, Ar), 142.9 (d, *J*_{C-F} = 3.7 Hz, C, Ar), 135.2 (d, *J*_{C-F} = 12.5 Hz, C, Ar), 124.2 (C, Ar), 120.9 (d, *J*_{C-F} = 10.0 Hz, CH, Ar), 108.1 (d, *J*_{C-F} = 24.3 Hz, CH, Ar), 96.3 (d, *J*_{C-F} = 26.3 Hz, CH, Ar), 95.6 (CH, Ar), 58.6 (C), 41.1 (CH₂), 34.3 (CH₂), 33.5 (CH₂), 29.6 (CH₂), 27.3 (CH₃); ESI-LRMS *m/z*: 259 [M + H]⁺; ESI-HRMS *m/z* calcd for M + H⁺ 259.1241, found: 259.1238.

10-Chloro-12b-methyl-1,5,6,12b-tetrahydropyrrolo[2',1':3,4]pyrazino[1,2-a]indol-3(2H)-one (SF9e): pale yellow oil (87.5 mg, yield 64%). ¹H-NMR (300 MHz, CDCl₃) δ 1.63 (s, 3H), 2.52–2.32 (m, 3H), 2.71–2.56 (m, 1H), 3.45–3.32 (m, 1H), 3.94–3.81 (m, 1H), 4.17 (dd, *J* = 11.6, 4.6 Hz, 1H), 4.52 (dd, *J* = 13.7, 5.0 Hz, 1H), 6.23 (s, 1H), 7.20–7.11 (m, 2H), 7.52 (s, 1H); ¹³C-NMR (100 MHz, CDCl₃) δ 173.1 (CO), 143.0 (C, Ar), 134.1 (C, Ar), 129.1 (C, Ar), 126.1 (C, Ar), 121.8 (CH, Ar), 119.9 (CH, Ar), 110.1 (CH, Ar), 96.0 (CH, Ar), 59.4 (C), 41.3 (CH₂), 34.8 (CH₂), 34.0 (CH₂), 30.2 (CH₂), 27.7 (CH₃); ESI-LRMS *m/z*: 277 ([M + H]⁺, Cl³⁷), 275 ([M + H]⁺, Cl³⁵); ESI-HRMS *m/z* calcd for M + H⁺ 275.0946, found: 275.0943. The characterization data is in accordance with that reported in [45].

13b-Methyl-2,3,6,7-tetrahydro-1H-pyrido[2',1':3,4]pyrazino[1,2-a]indol-4(13bH)-one (SF10a): white solid (73.5 mg, yield 58%), mp 113–114 °C. ¹H-NMR (500 MHz, DMSO-*d*₆) δ 1.67 (s, 3H), 1.78–1.69 (m, 1H), 1.98–1.88 (m, 1H), 2.07–1.99 (m, 1H), 2.42–2.26 (m, 3H), 3.40–3.25 (m, 1H), 3.81–3.70 (m, 1H), 4.33–4.24 (m, 1H), 4.95–4.85 (m, 1H), 6.34 (s, 1H), 7.06–7.01 (m, 1H), 7.14–7.07 (m, 1H), 7.37 (d, *J* = 8.1 Hz, 1H), 7.50 (d, *J* = 7.8 Hz, 1H); ¹³C-NMR (125 MHz, DMSO-*d*₆) δ 168.1 (CO), 142.4 (C, Ar), 135.1 (C, Ar), 127.7 (C, Ar), 120.6 (CH, Ar), 119.8 (CH, Ar), 119.7 (CH, Ar), 109.4 (CH, Ar), 95.2 (CH, Ar), 56.7 (C), 41.2 (CH₂), 36.6 (CH₂), 34.5 (CH₂), 31.7 (CH₂), 28.2 (CH₃), 16.9 (CH₂); ESI-LRMS *m/z*: 255 [M + H]⁺; ESI-HRMS *m/z* calcd for M + H⁺ 255.1492, found: 255.1488. The characterization data is in accordance with that reported in [43].

12,13b-Dimethyl-2,3,6,7-tetrahydro-1H-pyrido[2',1':3,4]pyrazino[1,2-a]indol-4(13bH)-one (SF10b): colorless oil (95.4 mg, yield 71%). ¹H-NMR (300 MHz, CDCl₃) δ 1.73 (s, 3H), 2.06–1.86 (m, 2H), 2.26–2.11 (m, 1H), 2.50–2.32 (m, 2H), 2.65–2.51 (m, 4H), 3.39–3.23 (m, 1H), 4.01–3.87 (m, 1H), 4.22–4.10 (m, 1H), 5.16 (dd, *J* = 13.7, 4.5 Hz, 1H), 6.26 (s, 1H), 6.99–6.88 (m, 1H), 7.18–7.07 (m, 2H); ¹³C-NMR (100 MHz, CDCl₃) δ 169.5 (CO), 141.4 (C, Ar), 135.2 (C, Ar), 129.9 (C, Ar), 127.9 (C, Ar), 121.6 (CH, Ar), 120.5 (CH, Ar), 106.6 (CH, Ar), 94.3 (CH, Ar), 57.4 (C), 41.7 (CH₂), 37.5 (CH₂), 35.3 (CH₂), 32.2 (CH₂), 28.9 (CH₃), 18.8 (CH₃), 17.4 (CH₂); ESI-LRMS *m/z*: 269 [M + H]⁺; ESI-HRMS *m/z* calcd for M + H⁺ 269.1648, found: 269.1645. The characterization data is in accordance with that reported in [45].

11-Chloro-13b-methyl-2,3,6,7-tetrahydro-1H-pyrido[2',1':3,4]pyrazino[1,2-a]indol-4(13bH)-one (SF10c): pale yellow oil (75.5 mg, yield 52%). ¹H-NMR (300 MHz, CDCl₃) δ 1.70 (s, 3H), 2.20–1.83 (m, 3H), 2.63–2.27 (m, 3H), 3.37–3.22 (m, 1H), 3.98–3.86 (m, 1H), 4.14 (dd, *J* = 11.6, 4.2 Hz, 1H), 5.16 (dd, *J* = 13.8, 4.2 Hz, 1H), 6.18 (s, 1H), 7.22–7.09 (m, 2H), 7.55–7.48 (m, 1H); ¹³C-NMR (100 MHz, CDCl₃) δ 169.4 (CO), 143.4 (C, Ar), 134.0 (C, Ar), 129.1 (C, Ar), 126.0 (C, Ar), 121.6 (CH, Ar), 119.8 (CH, Ar), 110.0 (CH, Ar), 95.5 (CH, Ar), 57.3 (C), 41.7 (CH₂), 37.4 (CH₂), 35.1 (CH₂), 32.1 (CH₂), 28.7 (CH₃), 17.3 (CH₂); ESI-LRMS *m/z*: 291 ([M + H]⁺, Cl³⁷), 289 ([M + H]⁺, Cl³⁵); ESI-HRMS *m/z* calcd for M + H⁺ 289.1102, found: 289.1099. The characterization data is in accordance with that reported in [45].

13b-Methyl-6,7-dihydroisindolo[1',2':3,4]pyrazino[1,2-a]indol-9(13bH)-one (SF11a): pale yellow solid (95.6 mg, yield 66%), mp 149–150 °C. ¹H-NMR (400 MHz, DMSO-*d*₆) δ 1.91 (s, 3H), 3.90–3.75 (m, 2H), 4.45–4.31 (m, 1H), 4.68–4.57 (m, 1H), 6.84 (s, 1H), 7.08–7.00 (m, 1H), 7.17–7.09 (m, 1H), 7.38 (d, *J* = 8.1 Hz,

1H), 7.59–7.48 (m, 2H), 7.80–7.69 (m, 2H), 8.24 (d, $J = 7.6$ Hz, 1H); ^{13}C -NMR (100 MHz, DMSO- d_6) δ 166.6 (CO), 150.3 (C, Ar), 137.8 (C, Ar), 135.2 (C, Ar), 132.8 (CH, Ar), 129.9 (C, Ar), 128.7 (CH, Ar), 127.3 (C, Ar), 123.1 (2 \times CH, Ar), 121.2 (CH, Ar), 120.0 (2 \times CH, Ar), 109.9 (CH, Ar), 97.8 (CH, Ar), 61.4 (C), 41.1 (CH₂), 34.2 (CH₂), 28.2 (CH₃); ESI-LRMS m/z : 289 [M + H]⁺; ESI-HRMS m/z calcd for M + H⁺ 289.1335, found: 289.1332. The characterization data is in accordance with that reported in [43].

15b-Methyl-8,9-dihydro-5H-indolo[2',1':3,4]pyrazino[2,1-a]isoquinolin-6(15bH)-one (SF12a): yellow solid (77.6 mg, yield 51%), mp 235–236 °C. ^1H -NMR (400 MHz, DMSO- d_6) δ 1.89 (s, 3H), 3.20–3.08 (m, 1H), 3.68 (d, $J = 19.5$ Hz, 1H), 3.81–3.72 (m, 1H), 4.10 (d, $J = 19.4$ Hz, 1H), 4.40–4.31 (m, 1H), 4.99–4.90 (m, 1H), 6.83 (s, 1H), 7.15–7.08 (m, 1H), 7.23–7.15 (m, 2H), 7.33–7.25 (m, 2H), 7.44–7.38 (m, 2H), 7.67 (d, $J = 7.7$ Hz, 1H); ^{13}C -NMR (125 MHz, DMSO- d_6) δ 168.3 (CO), 138.6 (C, Ar), 136.9 (C, Ar), 136.5 (C, Ar), 132.1 (C, Ar), 128.0 (CH, Ar), 127.6 (CH, Ar), 127.2 (C, Ar), 126.5 (CH, Ar), 124.2 (CH, Ar), 121.4 (CH, Ar), 120.3 (CH, Ar), 119.9 (CH, Ar), 109.7 (CH, Ar), 101.4 (CH, Ar), 61.8 (C), 42.8 (CH₂), 37.7 (CH₂), 37.4 (CH₂), 28.6 (CH₃); ESI-LRMS m/z : 303 [M + H]⁺; ESI-HRMS m/z calcd for M + H⁺ 303.1492, found: 303.1487. The characterization data is in accordance with that reported in [43].

13b-Methyl-5,6,7,13b-tetrahydro-1H-pyrrolo[2',1':3,4][1,4]diazepino[1,2-a]indol-3(2H)-one (SF13a): colorless oil (91.6 mg, yield 72%). ^1H -NMR (400 MHz, CDCl₃) δ 1.72 (s, 3H), 2.14–1.88 (m, 3H), 2.53–2.42 (m, 2H), 2.80–2.70 (m, 1H), 3.17–3.04 (m, 1H), 4.20 (ddd, $J = 14.8, 9.1, 2.5$ Hz, 1H), 4.56–4.33 (m, 2H), 6.45 (s, 1H), 7.13–7.06 (m, 1H), 7.24–7.19 (m, 1H), 7.30 (d, $J = 8.3$ Hz, 1H), 7.57 (d, $J = 7.8$ Hz, 1H); ^{13}C -NMR (100 MHz, CDCl₃) δ 174.2 (CO), 142.5 (C, Ar), 137.7 (C, Ar), 126.9 (C, Ar), 122.0 (CH, Ar), 120.7 (CH, Ar), 119.9 (CH, Ar), 109.0 (CH, Ar), 99.6 (CH, Ar), 62.4 (C), 43.4 (CH₂), 38.5 (CH₂), 35.0 (CH₂), 30.5 (CH₂), 28.0 (CH₂), 26.4 (CH₃); ESI-LRMS m/z : 255 [M + H]⁺; ESI-HRMS m/z calcd for M + H⁺ 255.1492, found: 255.1489. The characterization data is in accordance with that reported in [45].

11-Bromo-13b-methyl-5,6,7,13b-tetrahydro-1H-pyrrolo[2',1':3,4][1,4]diazepino[1,2-a]indol-3(2H)-one (SF13b): pale yellow oil (89.3 mg, yield 54%). ^1H -NMR (300 MHz, CDCl₃) δ 1.71 (s, 3H), 2.15–1.91 (m, 3H), 2.51–2.40 (m, 2H), 2.77–2.66 (m, 1H), 3.16–3.03 (m, 1H), 4.18 (ddd, $J = 14.8, 8.8, 2.7$ Hz, 1H), 4.46–4.32 (m, 2H), 6.37 (s, 1H), 7.14 (d, $J = 8.8$ Hz, 1H), 7.30–7.26 (m, 1H), 7.66 (d, $J = 1.9$ Hz, 1H); ^{13}C -NMR (100 MHz, CDCl₃) δ 174.1 (CO), 143.7 (C, Ar), 136.4 (C, Ar), 128.5 (C, Ar), 124.8 (CH, Ar), 123.1 (CH, Ar), 112.9 (C, Ar), 110.6 (CH, Ar), 99.1 (CH, Ar), 62.3 (C), 43.7 (CH₂), 38.5 (CH₂), 34.9 (CH₂), 30.4 (CH₂), 27.9 (CH₂), 26.3 (CH₃); ESI-LRMS m/z : 335 ([M + H]⁺, Br⁸¹), 333 ([M + H]⁺, Br⁷⁹); ESI-HRMS m/z calcd for M + H⁺ 333.0597, found: 333.0595. The characterization data is in accordance with that reported in [45].

12,13b-Dimethyl-5,6,7,13b-tetrahydro-1H-pyrrolo[2',1':3,4][1,4]diazepino[1,2-a]indol-3(2H)-one (SF13c): colorless oil (107.1 mg, yield 80%). ^1H -NMR (300 MHz, CDCl₃) δ 1.73 (s, 3H), 2.03–1.82 (m, 2H), 2.17–2.07 (m, 1H), 2.54–2.44 (m, 2H), 2.55 (s, 3H), 2.85–2.70 (m, 1H), 3.17–3.04 (m, 1H), 4.25–4.13 (m, 1H), 4.52–4.33 (m, 2H), 6.46 (s, 1H), 6.95–6.88 (m, 1H), 7.18–7.12 (m, 2H); ^{13}C -NMR (100 MHz, CDCl₃) δ 174.0 (CO), 141.8 (C, Ar), 137.3 (C, Ar), 130.1 (C, Ar), 126.5 (C, Ar), 122.1 (CH, Ar), 120.0 (CH, Ar), 106.6 (CH, Ar), 97.9 (CH, Ar), 62.3 (C), 43.5 (CH₂), 38.4 (CH₂), 34.8 (CH₂), 30.4 (CH₂), 28.0 (CH₂), 26.3 (CH₃), 18.6 (CH₃); ESI-LRMS m/z : 269 [M + H]⁺; ESI-HRMS m/z calcd for M + H⁺ 269.1648, found: 269.1644. The characterization data is in accordance with that reported in [45].

14b-Methyl-1,14b-dihydroindolo[1,2-a]pyrrolo[2,1-c]quinoxalin-3(2H)-one (SF14a): pale yellow solid (123.5 mg, yield 86%), mp 179–180 °C. ^1H -NMR (400 MHz, DMSO- d_6) δ 1.39 (s, 3H), 2.69–2.45 (m, 3H), 2.95–2.81 (m, 1H), 6.64 (s, 1H), 7.25–7.17 (m, 1H), 7.35–7.26 (m, 2H), 7.46–7.39 (m, 1H), 7.67 (d, $J = 7.7$ Hz, 1H), 8.13–8.04 (m, 2H), 8.16 (d, $J = 8.1$ Hz, 1H); ^{13}C -NMR (100 MHz, DMSO- d_6) δ 172.2 (CO), 142.7 (C, Ar), 133.1 (C, Ar), 129.3 (C, Ar), 128.8 (C, Ar), 125.8 (CH, Ar), 125.7 (C, Ar), 124.1 (CH, Ar), 123.0 (CH, Ar), 122.7 (CH, Ar), 121.4 (CH, Ar), 121.2 (CH, Ar), 117.2 (CH, Ar), 111.8 (CH, Ar), 97.6 (CH, Ar), 59.4 (C), 31.2 (CH₂), 30.0 (CH₂), 25.9 (CH₃); ESI-LRMS m/z : 289 [M + H]⁺; ESI-HRMS m/z calcd for M + H⁺ 289.1335, found: 289.1331. The characterization data is in accordance with that reported in [43].

2-Hexyl-14b-methyl-1,14b-dihydroindolo[1,2-a]pyrrolo[2,1-c]quinoxalin-3(2H)-one (SF14b): pale yellow oil (159.8 mg, yield 86% (dr = 1.5:1)), and the two diastereomers were inseparable by chromatography. ¹H-NMR (600 MHz, CDCl₃) δ 1.00–0.80 (m, 3.02H), 1.53–1.22 (m, 11.93H), 2.09–1.96 (m, 1.03H), 2.14–2.08 (m, 0.34H), 2.35–2.27 (m, 0.53H), 2.62–2.52 (m, 0.31H), 2.81–2.73 (m, 0.53H), 2.91–2.82 (m, 0.53H), 3.03–2.94 (m, 0.32H), 6.44 (s, 0.51H), 6.47 (s, 0.34H), 7.25–7.15 (m, 1.61H), 7.36–7.27 (m, 1.91H), 7.43–7.37 (m, 0.41H), 7.68–7.61 (m, 0.92H), 7.86 (dd, *J* = 7.9, 1.3 Hz, 0.34H), 8.06–7.95 (m, 1.91H), 8.28 (dd, *J* = 8.1, 1.4 Hz, 0.53H); ¹³C-NMR (150 MHz, CDCl₃) δ 175.3 (CO), 174.1 (CO), 143.4 (C, Ar), 141.9 (C, Ar), 134.4 (C, Ar), 133.6 (C, Ar), 130.6 (C, Ar), 129.8 (C, Ar), 129.5 (C, Ar), 129.4 (C, Ar), 126.4 (CH, Ar), 126.2 (C, Ar), 125.6 (CH, Ar), 125.4 (CH, Ar), 124.3 (2 × CH, Ar), 123.1 (2 × CH, Ar), 122.8 (CH, Ar), 121.6 (CH, Ar), 121.3 (2 × CH, Ar), 117.2 (CH, Ar), 117.1 (CH, Ar), 111.9 (CH, Ar), 111.7 (CH, Ar), 97.4 (CH, Ar), 97.1 (CH, Ar), 58.3 (C), 41.9 (CH), 41.5 (CH), 39.5 (CH₂), 37.7 (CH₂), 32.1 (CH₂), 31.9 (CH₂), 31.8 (CH₂), 30.9 (CH₂), 29.3 (CH₂), 29.3 (CH₂), 28.9 (CH₃), 27.6 (CH₂), 27.2 (CH₂), 26.2 (CH₃), 22.8 (CH₂), 22.7 (CH₂), 14.2 (2 × CH₃); ESI-LRMS *m/z*: 373 [M + H]⁺; ESI-HRMS *m/z* calcd for M + H⁺ 373.2274, found: 373.2273.

15b-Methyl-2,3-dihydro-1H-indolo[1,2-a]pyrido[2,1-c]quinoxalin-4(15bH)-one (SF15): pale yellow oil (89.4 mg, yield 59%). ¹H-NMR (400 MHz, DMSO-*d*₆) δ 1.29 (s, 3H), 1.97–1.75 (m, 2H), 2.42–2.28 (m, 2H), 2.71–2.56 (m, 2H), 6.60 (s, 1H), 7.23–7.17 (m, 1H), 7.33–7.24 (m, 2H), 7.47–7.40 (m, 1H), 7.71–7.64 (m, 2H), 8.08–8.01 (m, 2H); ¹³C-NMR (100 MHz, DMSO-*d*₆) δ 168.2 (CO), 142.5 (C, Ar), 133.2 (C, Ar), 130.5 (C, Ar), 129.1 (C, Ar), 128.4 (CH, Ar), 127.8 (C, Ar), 126.6 (CH, Ar), 123.4 (CH, Ar), 122.8 (CH, Ar), 121.2 (2 × CH, Ar), 116.9 (CH, Ar), 111.5 (CH, Ar), 96.8 (CH, Ar), 57.3 (C), 33.3 (CH₂), 32.9 (CH₂), 27.7 (CH₃), 17.1 (CH₂); ESI-LRMS *m/z*: 303 [M + H]⁺; ESI-HRMS *m/z* calcd for M + H⁺ 303.1492, found: 303.1486. The characterization data is in accordance with that reported in [43].

15b-Mmethylindolo[1,2-a]isoindolo[1,2-c]quinoxalin-11(15bH)-one (SF16): white solid (100.5 mg, yield 60%), mp 149–150 °C. ¹H-NMR (400 MHz, DMSO-*d*₆) δ 1.65 (s, 3H), 6.77 (s, 1H), 7.24–7.18 (m, 1H), 7.35–7.29 (m, 1H), 7.47–7.40 (m, 1H), 7.57–7.51 (m, 1H), 7.65 (d, *J* = 7.5 Hz, 1H), 7.76–7.68 (m, 1H), 7.96–7.87 (m, 2H), 8.04 (dd, *J* = 7.9, 1.5 Hz, 1H), 8.15 (d, *J* = 8.4 Hz, 1H), 8.31–8.26 (m, 1H), 8.35 (d, *J* = 7.6 Hz, 1H); ¹³C-NMR (100 MHz, DMSO-*d*₆) δ 164.1 (CO), 146.4 (C, Ar), 137.1 (C, Ar), 133.9 (C, Ar), 133.5 (CH, Ar), 129.7 (C, Ar), 129.5 (CH, Ar), 129.3 (C, Ar), 128.9 (C, Ar), 126.5 (CH, Ar), 124.6 (C, Ar), 124.4 (CH, Ar), 124.0 (CH, Ar), 123.9 (CH, Ar), 123.7 (CH, Ar), 123.5 (CH, Ar), 121.6 (CH, Ar), 121.3 (CH, Ar), 117.5 (CH, Ar), 111.9 (CH, Ar), 99.3 (CH, Ar), 61.2 (C), 26.3 (CH₃); ESI-LRMS *m/z*: 337 [M + H]⁺; ESI-HRMS *m/z* calcd for M + H⁺ 337.1335, found: 337.1329. The characterization data is in accordance with that reported in [43].

11b-Methyl-4,5-dihydro-3H-pyrrolo[3',2':3,4]pyrido[2,1-a]isoindol-7(11bH)-one (SF17): pale yellow solid (77.1 mg, yield 65%), mp 237–238 °C. ¹H-NMR (500 MHz, DMSO-*d*₆) δ 1.66 (s, 3H), 2.66–2.54 (m, 2H), 3.41–3.27 (m, 1H), 4.48–4.37 (m, 1H), 6.31–6.26 (m, 1H), 6.62–6.55 (m, 1H), 7.49–7.42 (m, 1H), 7.68–7.60 (m, 2H), 7.97 (d, *J* = 7.6 Hz, 1H), 10.56 (s, 1H); ¹³C-NMR (100 MHz, DMSO-*d*₆) δ 166.8 (CO), 152.2 (C, Ar), 131.9 (CH, Ar), 130.0 (C, Ar), 127.8 (CH, Ar), 122.7 (CH, Ar), 122.7 (C, Ar), 122.3 (CH, Ar), 119.9 (C, Ar), 116.8 (CH, Ar), 104.0 (CH, Ar), 62.3 (C), 34.5 (CH₂), 27.7 (CH₃), 22.6 (CH₂); ESI-LRMS *m/z*: 239 [M + H]⁺; ESI-HRMS *m/z* calcd for M + H⁺ 239.1179, found: 239.1175. The characterization data is in accordance with that reported in [43].

12b-Methyl-5,6-dihydropyrrolo[2',1':3,4]pyrazino[2,1-a]isoindol-8(12bH)-one (SF18): pale yellow solid (110.9 mg, yield 93%), mp 156–157 °C. ¹H-NMR (500 MHz, DMSO-*d*₆) δ 1.76 (s, 3H), 3.69–3.60 (m, 1H), 3.78–3.70 (m, 1H), 4.08 (dd, *J* = 12.0, 3.6 Hz, 1H), 4.45 (dd, *J* = 13.3, 4.2 Hz, 1H), 6.06–5.98 (m, 1H), 6.39–6.31 (m, 1H), 6.67–6.60 (m, 1H), 7.55–7.47 (m, 1H), 7.75–7.65 (m, 2H), 8.06 (d, *J* = 7.9 Hz, 1H); ¹³C-NMR (100 MHz, DMSO-*d*₆) δ 166.8 (CO), 151.1 (C, Ar), 132.6 (CH, Ar), 130.0 (C, Ar), 129.6 (C, Ar), 128.4 (CH, Ar), 122.9 (CH, Ar), 122.8 (CH, Ar), 119.4 (CH, Ar), 107.8 (CH, Ar), 104.2 (CH, Ar), 61.3 (C), 43.8 (CH₂), 34.9 (CH₂), 28.5 (CH₃); ESI-LRMS *m/z*: 239 [M + H]⁺; ESI-HRMS *m/z* calcd for M + H⁺ 239.1179, found: 239.1175. The characterization data is in accordance with that reported in [43].

9a-Methyl-4,5,9a-tetrahydrothieno[2,3-g]indolizin-7(8H)-one (SF19): pale yellow solid (65.1 mg, yield 63%), mp 128–129 °C. ¹H-NMR (400 MHz, DMSO-*d*₆) δ 1.42 (s, 3H), 1.90–1.79 (m, 1H), 2.31–2.15 (m, 2H), 2.61–2.52 (m, 1H), 2.74–2.62 (m, 1H), 2.85–2.76 (m, 1H), 3.09–2.98 (m, 1H), 4.15 (dd, *J* = 13.2, 5.6 Hz, 1H), 6.99 (d, *J* = 5.2 Hz, 1H), 7.37 (d, *J* = 5.1 Hz, 1H); ¹³C-NMR (100 MHz, DMSO-*d*₆) δ 171.6 (CO), 141.8 (C, Ar), 131.3 (C, Ar), 124.2 (CH, Ar), 124.1 (CH, Ar), 60.4 (C), 33.7 (CH₂), 33.4 (CH₂), 30.1 (CH₂), 25.8 (CH₃), 24.3 (CH₂); ESI-LRMS *m/z*: 208 [M + H]⁺; ESI-HRMS *m/z* calcd for M + H⁺ 208.0791, found: 208.0788. The characterization data is in accordance with that reported in [43].

11b-Methyl-4,5-dihydrothieno[3',2':3,4]pyridol[2,1-a]isoindol-7(11bH)-one (SF20): yellow solid (105.6 mg, yield 83%), mp 199–200 °C. ¹H-NMR (400 MHz, DMSO-*d*₆) δ 1.75 (s, 3H), 2.82–2.71 (m, 1H), 2.93–2.84 (m, 1H), 3.46–3.38 (m, 1H), 4.47 (dd, *J* = 13.4, 5.7 Hz, 1H), 7.39 (d, *J* = 5.3 Hz, 1H), 7.56–7.48 (m, 2H), 7.74–7.63 (m, 2H), 8.16 (d, *J* = 7.6 Hz, 1H); ¹³C-NMR (100 MHz, DMSO-*d*₆) δ 166.8 (CO), 150.2 (C, Ar), 137.8 (C, Ar), 132.8 (C, Ar), 132.3 (CH, Ar), 130.1 (C, Ar), 128.4 (CH, Ar), 125.3 (CH, Ar), 124.0 (CH, Ar), 123.0 (2 × CH, Ar), 63.4 (C), 34.7 (CH₂), 27.0 (CH₃), 24.8 (CH₂); ESI-LRMS *m/z*: 256 [M + H]⁺; ESI-HRMS *m/z* calcd for M + H⁺ 256.0791, found: 256.0785. The characterization data is in accordance with that reported in [43].

9a-Methyl-4,5,9a-tetrahydrothieno[3,2-g]indolizin-7(8H)-one (SF21): colorless oil (93.3 mg, yield 90%). ¹H-NMR (500 MHz, DMSO-*d*₆) δ 1.50 (s, 3H), 2.03–1.92 (m, 1H), 2.32–2.19 (m, 2H), 2.61–2.51 (m, 2H), 2.72–2.63 (m, 1H), 3.07–2.96 (m, 1H), 4.11 (dd, *J* = 13.3, 6.2 Hz, 1H), 6.80 (d, *J* = 5.1 Hz, 1H), 7.40 (d, *J* = 5.0 Hz, 1H); ¹³C-NMR (100 MHz, DMSO-*d*₆) δ 171.7 (CO), 141.8 (C, Ar), 132.3 (C, Ar), 127.1 (CH, Ar), 123.5 (CH, Ar), 60.4 (C), 35.1 (CH₂), 33.6 (CH₂), 30.2 (CH₂), 27.9 (CH₃), 25.1 (CH₂); ESI-LRMS *m/z*: 208 [M + H]⁺; ESI-HRMS *m/z* calcd for M + H⁺ 208.0791, found: 208.0788. The characterization data is in accordance with that reported in [43].

11b-Methyl-4,5-dihydrothieno[2',3':3,4]pyridol[2,1-a]isoindol-7(11bH)-one (SF22): pale yellow solid (108.6 mg, yield 85%), mp 137–138 °C. ¹H-NMR (500 MHz, DMSO-*d*₆) δ 1.82 (s, 3H), 2.62 (ddd, *J* = 16.2, 11.7, 6.5 Hz, 1H), 2.76 (dd, *J* = 16.2, 4.5 Hz, 1H), 3.40 (ddd, *J* = 13.4, 12.0, 4.7 Hz, 1H), 4.43 (dd, *J* = 13.5, 6.2 Hz, 1H), 6.82 (d, *J* = 5.1 Hz, 1H), 7.45 (d, *J* = 5.1 Hz, 1H), 7.57–7.49 (m, 1H), 7.76–7.67 (m, 2H), 7.97–7.90 (m, 1H); ¹³C-NMR (100 MHz, DMSO-*d*₆) δ 166.5 (CO), 150.2 (C, Ar), 138.0 (C, Ar), 133.4 (C, Ar), 132.5 (CH, Ar), 130.0 (C, Ar), 128.7 (CH, Ar), 127.1 (CH, Ar), 124.4 (CH, Ar), 123.1 (CH, Ar), 122.4 (CH, Ar), 63.1 (C), 34.3 (CH₂), 28.8 (CH₃), 25.6 (CH₂); ESI-LRMS *m/z*: 256 [M + H]⁺; ESI-HRMS *m/z* calcd for M + H⁺ 256.0791, found: 256.0789. The characterization data is in accordance with that reported in [43].

12b-Methyl-8,12b-dihydro-4H-thieno[2',3':3,4]pyridol[2,1-a]isoquinolin-7(5H)-one (SF23): pale yellow solid (63.4 mg, yield 47%), mp 155–156 °C. ¹H-NMR (500 MHz, DMSO-*d*₆) δ 1.87 (s, 3H), 2.50–2.44 (m, 1H), 2.76–2.68 (m, 1H), 3.10–2.99 (m, 1H), 3.64 (d, *J* = 20.3 Hz, 1H), 3.97 (d, *J* = 20.2 Hz, 1H), 4.90–4.79 (m, 1H), 6.91 (d, *J* = 5.1 Hz, 1H), 7.32–7.22 (m, 3H), 7.55 (d, *J* = 5.1 Hz, 1H), 7.77–7.71 (m, 1H); ¹³C-NMR (100 MHz, DMSO-*d*₆) δ 167.9 (CO), 139.0 (C, Ar), 138.8 (C, Ar), 136.4 (C, Ar), 131.3 (C, Ar), 128.0 (CH, Ar), 127.6 (CH, Ar), 127.4 (CH, Ar), 126.5 (CH, Ar), 124.8 (CH, Ar), 124.5 (CH, Ar), 62.6 (C), 37.0 (CH₂), 36.7 (CH₂), 31.7 (CH₃), 25.2 (CH₂); ESI-LRMS *m/z*: 270 [M + H]⁺; ESI-HRMS *m/z* calcd for M + H⁺ 270.0947, found: 270.0942. The characterization data is in accordance with that reported in [43].

8,9-Dimethoxy-10b-methyl-1,5,6,10b-tetrahydropyrrolo[2,1-a]isoquinolin-3(2H)-one (SF24a): white solid (114.5 mg, yield 88%), mp 53–54 °C. ¹H-NMR (500 MHz, DMSO-*d*₆) δ 1.45 (s, 3H), 1.93–1.82 (m, 1H), 2.25–2.15 (m, 1H), 2.45–2.37 (m, 1H), 2.59–2.47 (m, 1H), 2.70–2.62 (m, 2H), 3.05–2.96 (m, 1H), 3.71 (s, 3H), 3.75 (s, 3H), 4.08–4.00 (m, 1H), 6.66 (s, 1H), 6.78 (s, 1H); ¹³C-NMR (100 MHz, DMSO-*d*₆) δ 171.3 (CO), 147.7 (C, Ar), 147.4 (C, Ar), 134.9 (C, Ar), 124.1 (C, Ar), 111.9 (CH, Ar), 108.7 (CH, Ar), 60.3 (C), 55.8 (OCH₃), 55.5 (OCH₃), 34.3 (CH₂), 33.4 (CH₂), 30.2 (CH₂), 27.7 (CH₂), 26.8 (CH₃); ESI-LRMS *m/z*: 262 [M + H]⁺; ESI-HRMS *m/z* calcd for M + H⁺ 262.1438, found: 262.1434. The characterization data is in accordance with that reported in [43].

2-Hexyl-8,9-dimethoxy-10b-methyl-1,5,6,10b-tetrahydropyrrolo[2,1-a]isoquinolin-3(2H)-one (SF24b): white solid (81.2 mg, yield 47% (dr = 4:1)), mp 65–67 °C, and the two diastereomers were inseparable by

chromatography. $^1\text{H-NMR}$ (400 MHz, $\text{DMSO-}d_6$) δ 0.85–0.72 (m, 3H), 1.37–0.99 (m, 10H), 1.47–1.35 (m, 3H), 1.73–1.57 (m, 1H), 2.43–2.35 (m, 1H), 2.52–2.44 (m, 1H), 2.70–2.52 (m, 2H), 3.12–2.88 (m, 1H), 3.65–3.59 (m, 3H), 3.68 (s, 3H), 4.00–3.89 (m, 1H), 6.61–6.51 (m, 1H), 6.77–6.69 (m, 1H); $^{13}\text{C-NMR}$ (100 MHz, $\text{DMSO-}d_6$) δ 174.9 (CO), 147.5 (C, Ar), 147.4 (C, Ar), 134.7 (C, Ar), 124.4 (C, Ar), 112.0 (CH, Ar), 108.8 (CH, Ar), 59.5 (C, Ar), 55.7 (OCH₃), 55.4 (OCH₃), 41.2 (CH), 39.5 (CH₂), 34.2 (CH₂), 31.8 (CH₂), 31.2 (CH₂), 30.8 (CH₃), 28.6 (CH₂), 27.0 (CH₂), 26.9 (CH₂), 22.0 (CH₂), 14.0 (CH₃); ESI-LRMS m/z : 346 [M + H]⁺; ESI-HRMS m/z calcd for M + H⁺ 346.2377, found: 346.2375.

9,10-Dimethoxy-11b-methyl-2,3,6,7-tetrahydro-1H-pyrido[2,1-a]isoquinolin-4(11bH)-one (SF25): white solid (84.4 mg, yield 61%), mp 75–76 °C. $^1\text{H-NMR}$ (400 MHz, $\text{DMSO-}d_6$) δ 1.55 (s, 3H), 1.64–1.57 (m, 1H), 1.75–1.64 (m, 1H), 1.96–1.81 (m, 1H), 2.37–2.16 (m, 2H), 2.49–2.41 (m, 1H), 2.68–2.53 (m, 2H), 2.87–2.75 (m, 1H), 3.71 (s, 3H), 3.74 (s, 3H), 4.75–4.63 (m, 1H), 6.65 (s, 1H), 6.84 (s, 1H); $^{13}\text{C-NMR}$ (100 MHz, $\text{DMSO-}d_6$) δ 167.7 (CO), 147.4 (C, Ar), 147.2 (C, Ar), 135.2 (C, Ar), 125.5 (C, Ar), 111.7 (CH, Ar), 109.3 (CH, Ar), 58.2 (C), 55.8 (OCH₃), 55.4 (OCH₃), 36.7 (CH₂), 34.8 (CH₂), 31.5 (CH₂), 28.5 (CH₂), 27.3 (CH₃), 16.6 (CH₂); ESI-LRMS m/z : 276 [M + H]⁺; ESI-HRMS m/z calcd for M + H⁺ 276.1594, found: 276.1589. The characterization data is in accordance with that reported in [43].

2,3-Dimethoxy-12b-methyl-5,6-dihydroisoindolo[1,2-a]isoquinolin-8(12bH)-one (SF26): white solid (118.8 mg, yield 77%), mp 187–188 °C. $^1\text{H-NMR}$ (500 MHz, $\text{DMSO-}d_6$) δ 1.82 (s, 3H), 2.83–2.67 (m, 2H), 3.42–3.34 (m, 1H), 3.69 (s, 3H), 3.83 (s, 3H), 4.39–4.31 (m, 1H), 6.69 (s, 1H), 7.39 (s, 1H), 7.53–7.47 (m, 1H), 7.72–7.65 (m, 2H), 8.30 (d, $J = 7.7$ Hz, 1H); $^{13}\text{C-NMR}$ (125 MHz, $\text{DMSO-}d_6$) δ 166.5 (CO), 151.1 (C, Ar), 147.8 (C, Ar), 147.5 (C, Ar), 132.2 (CH, Ar), 130.8 (C, Ar), 130.3 (C, Ar), 128.3 (CH, Ar), 125.3 (C, Ar), 123.4 (CH, Ar), 122.8 (CH, Ar), 112.2 (CH, Ar), 110.2 (CH, Ar), 63.4 (C), 56.1 (OCH₃), 55.5 (OCH₃), 34.6 (CH₂), 28.7 (CH₂), 28.2 (CH₃); ESI-LRMS m/z : 310 [M + H]⁺; ESI-HRMS m/z calcd for M + H⁺ 310.1438, found: 310.1432. The characterization data is in accordance with that reported in [43].

3a-Methyl-2,3,3a,4-tetrahydropyrrolo[1,2-a]quinazoline-1,5-dione (SF27a): white solid (91.2 mg, yield 84%), mp 177–178 °C. $^1\text{H-NMR}$ (500 MHz, $\text{DMSO-}d_6$) δ 1.42 (s, 3H), 2.30–2.19 (m, 2H), 2.56–2.49 (m, 1H), 2.78–2.68 (m, 1H), 7.32–7.25 (m, 1H), 7.65–7.57 (m, 1H), 7.91 (dd, $J = 7.7, 1.4$ Hz, 1H), 8.07 (d, $J = 8.0$ Hz, 1H), 8.94 (s, 1H); $^{13}\text{C-NMR}$ (100 MHz, $\text{DMSO-}d_6$) δ 171.9 (CO), 161.2 (CO), 135.7 (C, Ar), 133.2 (CH, Ar), 127.7 (CH, Ar), 124.5 (CH, Ar), 119.9 (CH, Ar), 119.8 (C, Ar), 74.0 (C), 32.4 (CH₂), 29.6 (CH₂), 26.4 (CH₃); ESI-LRMS m/z : 217 [M + H]⁺; ESI-HRMS m/z calcd for M + H⁺ 217.0972, found: 217.0969. The characterization data is in accordance with that reported in [43].

3a,4-Dimethyl-2,3,3a,4-tetrahydropyrrolo[1,2-a]quinazoline-1,5-dione (SF27b): white solid (97.5 mg, yield 85%), mp 105–107 °C. $^1\text{H-NMR}$ (600 MHz, CDCl_3) δ 1.46 (s, 3H), 2.30 (ddd, $J = 12.0, 6.1, 4.0$ Hz, 1H), 2.48–2.39 (m, 1H), 2.70–2.63 (m, 2H), 3.07 (s, 3H), 7.27–7.24 (m, 1H), 7.56–7.51 (m, 1H), 8.08 (dd, $J = 7.8, 1.6$ Hz, 1H), 8.26 (dd, $J = 8.2, 0.8$ Hz, 1H); $^{13}\text{C-NMR}$ (150 MHz, CDCl_3) δ 171.3 (CO), 162.1 (CO), 135.2 (C, Ar), 133.4 (CH, Ar), 128.6 (CH, Ar), 125.0 (CH, Ar), 119.7 (CH, Ar), 119.4 (C, Ar), 78.5 (C), 32.4 (CH₂), 30.3 (CH₂), 27.8 (CH₃), 21.8 (CH₃); ESI-LRMS m/z : 231 [M + H]⁺; ESI-HRMS m/z calcd for M + H⁺ 231.1128, found: 231.1127. The characterization data is in accordance with that reported in [43].

4a-Methyl-3,4,4a,5-tetrahydro-1H-pyrido[1,2-a]quinazoline-1,6(2H)-dione (SF28a): white solid (70.7 mg, yield 61%), mp 198–199 °C. $^1\text{H-NMR}$ (500 MHz, $\text{DMSO-}d_6$) δ 1.35 (s, 3H), 1.90–1.74 (m, 2H), 2.09–2.02 (m, 1H), 2.17–2.09 (m, 1H), 2.48–2.39 (m, 1H), 2.62–2.54 (m, 1H), 7.36–7.28 (m, 1H), 7.60–7.52 (m, 1H), 7.66 (d, $J = 8.0$ Hz, 1H), 7.86 (dd, $J = 7.7, 1.4$ Hz, 1H), 8.85 (s, 1H); $^{13}\text{C-NMR}$ (100 MHz, $\text{DMSO-}d_6$) δ 168.8 (CO), 162.3 (CO), 138.1 (C, Ar), 131.8 (CH, Ar), 126.5 (CH, Ar), 126.2 (CH, Ar), 125.2 (CH, Ar), 123.7 (C, Ar), 71.1 (C), 34.7 (CH₂), 33.1 (CH₂), 28.3 (CH₃), 16.6 (CH₂); ESI-LRMS m/z : 231 [M + H]⁺; ESI-HRMS m/z calcd for M + H⁺ 231.1128, found: 231.1126. The characterization data is in accordance with that reported in [43].

4a,5-Dimethyl-3,4,4a,5-tetrahydro-1H-pyrido[1,2-a]quinazoline-1,6(2H)-dione (SF28b): white solid (78.3 mg, yield 64%), mp 138–139 °C. $^1\text{H-NMR}$ (600 MHz, CDCl_3) δ 1.39 (s, 3H), 1.98–1.86 (m, 2H), 2.17–2.10 (m, 1H), 2.44–2.36 (m, 1H), 2.63–2.55 (m, 1H), 2.74–2.65 (m, 1H), 3.12 (s, 3H), 7.32–7.28 (m, 1H), 7.54–7.49

(m, 1H), 7.62 (dd, $J = 8.1, 0.9$ Hz, 1H), 8.02 (dd, $J = 7.8, 1.6$ Hz, 1H); ^{13}C -NMR (150 MHz, CDCl_3) δ 169.3 (CO), 163.6 (CO), 137.4 (C, Ar), 132.0 (CH, Ar), 127.8 (CH, Ar), 126.2 (CH, Ar), 126.0 (CH, Ar), 123.9 (C, Ar), 75.5 (C), 34.4 (CH_2), 33.7 (CH_2), 27.5 (CH_3), 24.6 (CH_3), 16.9 (CH_2); ESI-LRMS m/z : 245 [$\text{M} + \text{H}$] $^+$; ESI-HRMS m/z calcd for $\text{M} + \text{H}^+$ 245.1285, found: 245.1284. The characterization data is in accordance with that reported in [43].

6a-Methyl-6,6a-dihydroisoindolo[2,1-a]quinazoline-5,11-dione (SF29a): white solid (99.3 mg, yield 75%), mp 219–220 °C. ^1H -NMR (400 MHz, $\text{DMSO}-d_6$) δ 1.72 (s, 3H), 7.42–7.36 (m, 1H), 7.70–7.64 (m, 1H), 7.77–7.71 (m, 1H), 7.85–7.78 (m, 1H), 7.89 (d, $J = 7.5$ Hz, 1H), 7.95 (d, $J = 7.6$ Hz, 1H), 8.04–7.98 (m, 2H), 9.48 (s, 1H); ^{13}C -NMR (100 MHz, $\text{DMSO}-d_6$) δ 164.4 (CO), 162.5 (CO), 146.0 (C, Ar), 135.2 (C, Ar), 133.7 (CH, Ar), 133.6 (CH, Ar), 130.1 (CH, Ar), 129.4 (C, Ar), 128.0 (CH, Ar), 125.1 (CH, Ar), 124.0 (CH, Ar), 122.9 (CH, Ar), 121.2 (CH, Ar), 119.8 (C, Ar), 74.2 (C), 27.3 (CH_3); ESI-LRMS m/z : 265 [$\text{M} + \text{H}$] $^+$; ESI-HRMS m/z calcd for $\text{M} + \text{H}^+$ 265.0972, found: 265.0966. The characterization data is in accordance with that reported in [43].

6,6a-Dimethyl-6,6a-dihydroisoindolo[2,1-a]quinazoline-5,11-dione (SF29b): white solid (97.1 mg, yield 70%), mp 182–184 °C. ^1H -NMR (600 MHz, CDCl_3) δ 1.72 (s, 3H), 3.25 (s, 3H), 7.37–7.32 (m, 1H), 7.67–7.63 (m, 2H), 7.76–7.70 (m, 2H), 8.05–7.99 (m, 2H), 8.15 (dd, $J = 8.1, 1.0$ Hz, 1H); ^{13}C -NMR (150 MHz, CDCl_3) δ 165.0 (CO), 163.0 (CO), 143.3 (C, Ar), 134.8 (C, Ar), 133.5 (CH, Ar), 132.8 (CH, Ar), 131.4 (C, Ar), 130.5 (CH, Ar), 128.9 (CH, Ar), 125.5 (CH, Ar), 125.2 (CH, Ar), 124.6 (CH, Ar), 121.8 (CH, Ar), 120.6 (C, Ar), 78.1 (C), 29.6 (CH_3), 23.3 (CH_3); ESI-LRMS m/z : 279 [$\text{M} + \text{H}$] $^+$; ESI-HRMS m/z calcd for $\text{M} + \text{H}^+$ 279.1128, found: 279.1127. The characterization data is in accordance with that reported in [43].

4b-Methyl-4bH-isoquinolino[2,1-a]quinazoline-6,12(5H,13H)-dione (SF30a): yellow solid (91.5 mg, yield 66%), mp 225–226 °C. ^1H -NMR (400 MHz, $\text{DMSO}-d_6$) δ 1.71 (s, 3H), 3.84 (d, $J = 21.2$ Hz, 1H), 4.16 (d, $J = 21.1$ Hz, 1H), 7.30–7.23 (m, 1H), 7.45–7.36 (m, 3H), 7.68–7.61 (m, 1H), 7.79–7.71 (m, 1H), 7.82 (d, $J = 7.8$ Hz, 1H), 7.93 (dd, $J = 7.7, 1.5$ Hz, 1H), 8.89 (s, 1H); ^{13}C -NMR (100 MHz, $\text{DMSO}-d_6$) δ 165.5 (CO), 161.9 (CO), 137.6 (C, Ar), 133.1 (C, Ar), 132.1 (CH, Ar), 128.8 (CH, Ar), 128.6 (C, Ar), 127.5 (CH, Ar), 127.2 (CH, Ar), 126.6 (CH, Ar), 126.2 (CH, Ar), 126.1 (CH, Ar), 125.7 (CH, Ar), 123.3 (C, Ar), 73.9 (C), 35.2 (CH_2), 30.5 (CH_3); ESI-LRMS m/z : 279 [$\text{M} + \text{H}$] $^+$; ESI-HRMS m/z calcd for $\text{M} + \text{H}^+$ 279.1128, found: 279.1122. The characterization data is in accordance with that reported in [43].

4b,5-Dimethyl-4bH-isoquinolino[2,1-a]quinazoline-6,12(5H,13H)-dione (SF30b): yellow oil (29.1 mg, yield 20%). ^1H -NMR (600 MHz, CDCl_3) δ 1.86 (s, 3H), 2.77 (s, 3H), 3.91 (s, 2H), 7.28 (d, $J = 7.5$ Hz, 1H), 7.45–7.39 (m, 2H), 7.49–7.45 (m, 1H), 7.61–7.55 (m, 2H), 7.63 (d, $J = 8.0$ Hz, 1H), 8.08 (dd, $J = 7.9, 1.3$ Hz, 1H); ^{13}C -NMR (150 MHz, $\text{DMSO}-d_6$) δ 169.2 (CO), 162.1 (CO), 138.6 (C, Ar), 131.9 (CH, Ar), 131.8 (C, Ar), 130.6 (C, Ar), 129.9 (CH, Ar), 128.9 (CH, Ar), 128.0 (CH, Ar), 127.7 (CH, Ar), 127.0 (CH, Ar), 126.9 (CH, Ar), 126.7 (CH, Ar), 125.2 (C, Ar), 76.7 (C), 36.2 (CH_2), 29.9 (CH_3), 25.7 (CH_3); ESI-LRMS m/z : 293 [$\text{M} + \text{H}$] $^+$; ESI-HRMS m/z calcd for $\text{M} + \text{H}^+$ 293.1285, found: 293.1284.

3a-Methyl-2,3,3a,4-tetrahydropyrrolo[2,1-b]quinazolin-1(9H)-one (SF31): white solid (69.4 mg, yield 69%), mp 141–143 °C. ^1H -NMR (600 MHz, CDCl_3) δ 1.54 (s, 3H), 2.15–2.05 (m, 2H), 2.52–2.45 (m, 1H), 2.60–2.52 (m, 1H), 4.17 (d, $J = 16.7$ Hz, 1H), 5.02 (d, $J = 16.8$ Hz, 1H), 6.58 (dd, $J = 8.0, 0.8$ Hz, 1H), 6.81–6.76 (m, 1H), 7.07–6.99 (m, 2H); ^{13}C -NMR (150 MHz, CDCl_3) δ 174.3 (CO), 141.9 (C, Ar), 127.6 (CH, Ar), 127.0 (CH, Ar), 119.3 (CH, Ar), 117.4 (C, Ar), 116.5 (CH, Ar), 71.9 (C), 38.6 (CH_2), 33.0 (CH_2), 29.6 (CH_2), 25.6 (CH_3); ESI-LRMS m/z : 203 [$\text{M} + \text{H}$] $^+$; ESI-HRMS m/z calcd for $\text{M} + \text{H}^+$ 203.1179, found: 203.1178. The characterization data is in accordance with that reported in [43].

4b-Methyl-4b,5-dihydroisoindolo[1,2-b]quinazolin-12(10H)-one (SF32): pale yellow solid (41.1 mg, yield 33%), mp 222–223 °C. ^1H -NMR (600 MHz, CDCl_3) δ 1.71 (s, 3H), 4.24 (s, 1H), 4.45 (d, $J = 16.9$ Hz, 1H), 5.32 (d, $J = 17.0$ Hz, 1H), 6.69 (d, $J = 8.3$ Hz, 1H), 6.90–6.85 (m, 1H), 7.12–7.08 (m, 1H), 7.14 (d, $J = 7.5$ Hz, 1H), 7.56–7.52 (m, 1H), 7.63 (d, $J = 3.9$ Hz, 2H), 7.88 (d, $J = 7.6$ Hz, 1H); ^{13}C -NMR (150 MHz, CDCl_3) δ 165.8 (CO), 147.8 (C, Ar), 140.2 (C, Ar), 132.3 (CH, Ar), 131.5 (C, Ar), 129.6 (CH, Ar), 127.9 (CH, Ar), 127.2 (CH, Ar), 124.4 (CH, Ar), 120.7 (CH, Ar), 120.5 (CH, Ar), 118.7 (C, Ar), 118.1 (CH, Ar), 71.5

(C), 38.0 (CH₂), 23.9 (CH₃); ESI-LRMS *m/z*: 251 [M + H]⁺; ESI-HRMS *m/z* calcd for M + H⁺ 251.1179, found: 251.1178. The characterization data is in accordance with that reported in [43].

3a-Methyl-2,3,3a,4-tetrahydro-1H-benzo[d]pyrrolo[1,2-a]imidazol-1-one (SF33): colorless oil (45.1 mg, yield 48%). ¹H-NMR (600 MHz, CDCl₃) δ 1.51 (s, 3H), 2.44–2.33 (m, 2H), 2.54 (ddd, *J* = 16.8, 8.5, 1.6 Hz, 1H), 2.78 (ddd, *J* = 16.8, 11.7, 8.5 Hz, 1H), 6.68 (dd, *J* = 7.7, 0.7 Hz, 1H), 6.84–6.79 (m, 1H), 6.98–6.93 (m, 1H), 7.43 (dd, *J* = 7.6, 1.1 Hz, 1H); ¹³C-NMR (150 MHz, CDCl₃) δ 173.9 (CO), 142.8 (C, Ar), 128.7 (C, Ar), 125.4 (CH, Ar), 120.3 (CH, Ar), 115.5 (CH, Ar), 110.7 (CH, Ar), 85.7 (C), 37.8 (CH₂), 33.7 (CH₂), 26.3 (CH₃); ESI-LRMS *m/z*: 189 [M + H]⁺; ESI-HRMS *m/z* calcd for M + H⁺ 189.1022, found: 189.1023. The characterization data is in accordance with that reported in [34].

12a-Methyl-12,12a-dihydrobenzo[4,5]imidazo[2,1-a]isoquinolin-6(5H)-one (SF34): colorless oil (26.1 mg, yield 21%). ¹H-NMR (600 MHz, CDCl₃) δ 1.69 (s, 3H), 3.71 (d, *J* = 19.0 Hz, 1H), 3.88 (d, *J* = 19.0 Hz, 1H), 4.48 (s, 1H), 6.85 (dd, *J* = 7.6, 0.5 Hz, 1H), 6.93–6.89 (m, 1H), 7.02–6.97 (m, 1H), 7.24 (d, *J* = 7.5 Hz, 1H), 7.33–7.30 (m, 1H), 7.37–7.33 (m, 1H), 7.41 (dd, *J* = 7.6, 0.9 Hz, 1H), 8.02–7.98 (m, 1H); ¹³C-NMR (150 MHz, CDCl₃) δ 165.5 (CO), 139.3 (C, Ar), 139.1 (C, Ar), 131.3 (C, Ar), 129.8 (C, Ar), 128.4 (CH, Ar), 128.0 (CH, Ar), 127.6 (CH, Ar), 125.0 (CH, Ar), 123.2 (CH, Ar), 121.6 (CH, Ar), 116.6 (CH, Ar), 112.0 (CH, Ar), 82.3 (C), 38.7 (CH₂), 29.5 (CH₃); ESI-LRMS *m/z*: 251 [M + H]⁺; ESI-HRMS *m/z* calcd for M + H⁺ 251.1179, found: 251.1178. The characterization data is in accordance with that reported in [43].

3a-Methyl-3,3a-dihydro-1H-benzo[d]pyrrolo[2,1-b][1,3]oxazine-1,5(2H)-dione (SF35a): white solid (98.9 mg, yield 91%), mp 114–115 °C. ¹H-NMR (400 MHz, DMSO-*d*₆) δ 1.63 (s, 3H), 2.48–2.41 (m, 2H), 2.68–2.59 (m, 1H), 2.82–2.71 (m, 1H), 7.44–7.36 (m, 1H), 7.83–7.76 (m, 1H), 8.08–7.92 (m, 2H); ¹³C-NMR (125 MHz, DMSO-*d*₆) δ 171.7 (CO), 161.1 (CO), 136.1 (C, Ar), 135.7 (CH, Ar), 129.9 (CH, Ar), 125.5 (CH, Ar), 120.5 (CH, Ar), 115.7 (C, Ar), 95.4 (C), 31.7 (CH₂), 29.1 (CH₂), 24.0 (CH₃); ESI-LRMS *m/z*: 218 [M + H]⁺; ESI-HRMS *m/z* calcd for M + H⁺ 218.0812, found: 218.0809. The characterization data is in accordance with that reported in [43].

2-Hexyl-3a-methyl-3,3a-dihydro-1H-benzo[d]pyrrolo[2,1-b][1,3]oxazine-1,5(2H)-dione (SF35b): colorless oil (75.4 mg, yield 50% (dr = 5.5:1)), and the two diastereomers were inseparable by chromatography. ¹H-NMR (600 MHz, DMSO-*d*₆) for the major isomer: δ 0.91–0.84 (m, 3H), 1.42–1.21 (m, 9H), 1.65–1.61 (m, 3H), 1.85–1.78 (m, 1H), 2.13–2.07 (m, 1H), 2.71–2.62 (m, 1H), 2.91–2.83 (m, 1H), 7.41–7.37 (m, 1H), 7.81–7.78 (m, 1H), 8.00 (dd, *J* = 7.8, 1.5 Hz, 1H), 8.10–8.07 (m, 1H); ¹³C-NMR (150 MHz, DMSO-*d*₆) for major isomer: δ 173.0 (CO), 161.0 (CO), 136.0 (CH, Ar), 135.8 (CH, Ar), 129.9 (CH, Ar), 125.3 (CH, Ar), 119.8 (CH, Ar), 115.1 (C, Ar), 93.5 (C, Ar), 39.8 (CH), 38.5 (CH₂), 31.2 (CH₂), 29.6 (CH₂), 28.6 (CH₂), 26.3 (CH₂), 23.5 (CH₃), 22.1 (CH₂), 14.0 (CH₃); ESI-LRMS *m/z*: 302 [M + H]⁺; ESI-HRMS *m/z* calcd for M + H⁺ 302.1751, found: 302.1750.

4a-Methyl-2,3,4,4a-tetrahydrobenzo[d]pyrido[2,1-b][1,3]oxazine-1,6-dione (SF36): colorless oil (88.5 mg, yield 77%). ¹H-NMR (500 MHz, DMSO-*d*₆) δ 1.55 (s, 3H), 1.86–1.77 (m, 1H), 1.95–1.86 (m, 1H), 2.31–2.21 (m, 2H), 2.55–2.48 (m, 1H), 2.68–2.58 (m, 1H), 7.46–7.39 (m, 1H), 7.77–7.70 (m, 2H), 7.98–7.93 (m, 1H); ¹³C-NMR (125 MHz, DMSO-*d*₆) δ 169.0 (CO), 161.8 (CO), 138.6 (C, Ar), 134.1 (CH, Ar), 128.7 (CH, Ar), 126.1 (2 × CH, Ar), 119.9 (C, Ar), 92.7 (C), 34.9 (CH₂), 32.9 (CH₂), 25.9 (CH₃), 16.1 (CH₂); ESI-LRMS *m/z*: 232 [M + H]⁺; ESI-HRMS *m/z* calcd for M + H⁺ 232.0968, found: 232.0965. The characterization data is in accordance with that reported in ref.43. The characterization data is in accordance with that reported in [43].

6a-Methyl-5H-benzo[4,5][1,3]oxazino[2,3-a]isoindole-5,11(6aH)-dione (SF37): pale yellow solid (83.6 mg, yield 63%), mp 138–139 °C. ¹H-NMR (400 MHz, DMSO-*d*₆) δ 1.94 (s, 3H), 7.51–7.45 (m, 1H), 7.79–7.73 (m, 1H), 7.93–7.85 (m, 2H), 7.95 (d, *J* = 7.5 Hz, 1H), 8.06–8.00 (m, 2H), 8.08 (dd, *J* = 7.8, 1.2 Hz, 1H); ¹³C-NMR (125 MHz, DMSO-*d*₆) δ 164.1 (CO), 161.3 (CO), 143.8 (C, Ar), 136.0 (CH, Ar), 135.7 (C, Ar), 134.4 (CH, Ar), 131.3 (CH, Ar), 130.2 (CH, Ar), 129.4 (C, Ar), 125.7 (CH, Ar), 124.2 (CH, Ar), 123.2 (CH, Ar), 121.2 (CH, Ar), 115.3 (C, Ar), 92.5 (C), 23.4 (CH₃); ESI-LRMS *m/z*: 266 [M + H]⁺; ESI-HRMS

m/z calcd for $M + H^+$ 266.0812, found: 266.0807. The characterization data is in accordance with that reported in [43].

3a-Methyl-3,3a-dihydro-1H-naphtho[2,3-d]pyrrolo[2,1-b][1,3]oxazine-1,5(2H)-dione (SF38): yellow solid (128.1 mg, yield 96%), mp 228–230 °C. $^1\text{H-NMR}$ (600 MHz, CDCl_3) δ 1.72 (s, 3H), 2.50–2.42 (m, 1H), 2.68–2.61 (m, 1H), 2.76–2.68 (m, 1H), 2.84–2.77 (m, 1H), 7.56–7.51 (m, 1H), 7.67–7.62 (m, 1H), 7.91 (d, $J = 8.3$ Hz, 1H), 7.95 (d, $J = 8.2$ Hz, 1H), 8.44 (s, 1H), 8.72 (s, 1H); $^{13}\text{C-NMR}$ (150 MHz, CDCl_3) δ 171.7 (CO), 162.3 (CO), 136.7 (C, Ar), 133.2 (CH, Ar), 131.1 (C, Ar), 130.5 (C, Ar), 129.9 (CH, Ar), 129.7 (CH, Ar), 128.0 (CH, Ar), 126.9 (CH, Ar), 119.4 (CH, Ar), 115.7 (C, Ar), 95.7 (C), 32.3 (CH_2), 29.6 (CH_2), 25.7 (CH_3); ESI-LRMS m/z : 268 [$M + H$] $^+$; ESI-HRMS m/z calcd for $M + H^+$ 268.0968, found: 268.0962. The characterization data is in accordance with that reported in [35].

4a-Methyl-2,3,4,4a-tetrahydronaphtho[2,3-d]pyrido[2,1-b][1,3]oxazine-1,6-dione (SF39): pale yellow oil (103.7 mg, yield 74%). $^1\text{H-NMR}$ (600 MHz, CDCl_3) δ 1.64 (s, 3H), 1.94–1.87 (m, 1H), 2.22–2.12 (m, 2H), 2.52–2.46 (m, 1H), 2.74–2.61 (m, 2H), 7.57–7.53 (m, 1H), 7.66–7.61 (m, 1H), 7.90 (d, $J = 8.3$ Hz, 1H), 7.96 (d, $J = 8.2$ Hz, 1H), 8.22 (s, 1H), 8.67 (s, 1H); $^{13}\text{C-NMR}$ (150 MHz, CDCl_3) δ 169.3 (CO), 163.3 (CO), 135.9 (C, Ar), 133.0 (C, Ar), 131.8 (CH, Ar), 130.8 (C, Ar), 129.6 (CH, Ar), 129.5 (CH, Ar), 128.2 (CH, Ar), 127.1 (CH, Ar), 124.9 (CH, Ar), 119.2 (C, Ar), 92.5 (C), 36.3 (CH_2), 33.7 (CH_2), 27.7 (CH_3), 16.7 (CH_2); ESI-LRMS m/z : 282 [$M + H$] $^+$; ESI-HRMS m/z calcd for $M + H^+$ 282.1125, found: 282.1117. The characterization data is in accordance with that reported in [43].

4b-Methyl-4bH-naphtho[2',3':4,5][1,3]oxazino[2,3-a]isoindole-6,14-dione (SF40): white solid (113.2 mg, yield 72%), mp 210–212 °C. $^1\text{H-NMR}$ (600 MHz, CDCl_3) δ 1.98 (s, 3H), 7.58–7.54 (m, 1H), 7.69–7.64 (m, 2H), 7.78–7.74 (m, 1H), 7.81–7.79 (m, 1H), 8.02–7.95 (m, 3H), 8.49 (s, 1H), 8.79 (s, 1H); $^{13}\text{C-NMR}$ (150 MHz, CDCl_3) δ 164.7 (CO), 162.4 (CO), 144.0 (C, Ar), 136.9 (C, Ar), 133.9 (CH, Ar), 133.5 (CH, Ar), 131.1 (CH, Ar), 130.9 (C, Ar), 130.4 (C, Ar), 130.3 (C, Ar), 130.0 (CH, Ar), 129.9 (CH, Ar), 128.0 (CH, Ar), 126.8 (CH, Ar), 124.8 (CH, Ar), 122.6 (CH, Ar), 119.4 (CH, Ar), 115.0 (C, Ar), 92.7 (C), 25.0 (CH_3); ESI-LRMS m/z : 316 [$M + H$] $^+$; ESI-HRMS m/z calcd for $M + H^+$ 316.0968, found: 316.0959. The characterization data is in accordance with that reported in [43].

6a-Methyl-7,8-dihydro-5H-pyrido[2,3-d]pyrrolo[2,1-b][1,3]oxazine-5,9(6aH)-dione (SF41): colorless oil (65.1 mg, yield 60%). $^1\text{H-NMR}$ (600 MHz, CDCl_3) δ 1.72 (s, 3H), 2.52–2.41 (m, 1H), 2.68–2.60 (m, 1H), 2.86–2.69 (m, 2H), 7.36 (dd, $J = 7.7, 4.9$ Hz, 1H), 8.42 (dd, $J = 7.7, 1.9$ Hz, 1H), 8.81 (dd, $J = 4.9, 1.9$ Hz, 1H); $^{13}\text{C-NMR}$ (150 MHz, CDCl_3) δ 171.6 (CO), 161.3 (CO), 155.1 (CH, Ar), 149.1 (C, Ar), 139.4 (CH, Ar), 122.0 (CH, Ar), 113.0 (C, Ar), 96.1 (C), 32.3 (CH_2), 29.8 (CH_2), 25.4 (CH_3); ESI-LRMS m/z : 219 [$M + H$] $^+$; ESI-HRMS m/z calcd for $M + H^+$ 219.0764, found: 219.0763. The characterization data is in accordance with that reported in [35].

3a-Methyl-2,3,3a,5-tetrahydro-1H-benzo[d]pyrrolo[2,1-b][1,3]oxazin-1-one (SF42): pale yellow oil (33.8 mg, yield 33%). $^1\text{H-NMR}$ (500 MHz, $\text{DMSO-}d_6$) δ 1.45 (s, 3H), 2.07–1.97 (m, 1H), 2.29–2.19 (m, 1H), 2.43 (ddd, $J = 17.1, 10.0, 2.1$ Hz, 1H), 2.76–2.65 (m, 1H), 4.88 (d, $J = 16.0$ Hz, 1H), 4.99 (d, $J = 16.0$ Hz, 1H), 7.16–7.10 (m, 1H), 7.21–7.16 (m, 1H), 7.32–7.25 (m, 1H), 8.20 (d, $J = 8.1$ Hz, 1H); $^{13}\text{C-NMR}$ (125 MHz, $\text{DMSO-}d_6$) δ 170.9 (CO), 132.6 (C, Ar), 127.1 (CH, Ar), 124.7 (CH, Ar), 123.7 (CH, Ar), 123.2 (C, Ar), 119.2 (CH, Ar), 89.6 (C), 62.0 (CH_2), 32.5 (CH_2), 29.7 (CH_2), 20.7 (CH_3); ESI-LRMS m/z : 204 [$M + H$] $^+$; ESI-HRMS m/z calcd for $M + H^+$ 204.1019, found: 204.1017. The characterization data is in accordance with that reported in [43].

6a-Methyl-5H-benzo[4,5][1,3]oxazino[2,3-a]isoindol-11(6aH)-one (SF43): colorless oil (22.4 mg, yield 18%). $^1\text{H-NMR}$ (600 MHz, CDCl_3) δ 1.74 (s, 3H), 4.98 (d, $J = 15.3$ Hz, 1H), 5.20 (d, $J = 15.3$ Hz, 1H), 7.14–7.10 (m, 1H), 7.19–7.15 (m, 1H), 7.40–7.35 (m, 1H), 7.59–7.54 (m, 1H), 7.68–7.60 (m, 2H), 7.91 (d, $J = 7.5$ Hz, 1H), 8.25 (d, $J = 8.2$ Hz, 1H); $^{13}\text{C-NMR}$ (150 MHz, CDCl_3) δ 165.2 (CO), 146.1 (C, Ar), 133.1 (CH, Ar), 132.6 (C, Ar), 131.2 (C, Ar), 130.2 (CH, Ar), 127.9 (CH, Ar), 124.3 (2 \times CH, Ar), 124.2 (CH, Ar), 123.0 (C, Ar), 121.8 (CH, Ar), 121.5 (CH, Ar), 88.1 (C), 63.3 (CH_2), 20.8 (CH_3); ESI-LRMS m/z : 252 [$M + H$] $^+$;

ESI-HRMS m/z calcd for $M + H^+$ 252.1019, found: 252.1018. The characterization data is in accordance with that reported in [43].

3.4. General Procedure of the Reductive Preparation of Compounds SF47–SF55

To a solution of substrates (0.3 mmol) in dry THF was added $AlCl_3$ (0.6 mmol), then $LiAlH_4$ (0.6 mmol) was added portionwise at 0 °C. After that, the mixture was heated to reflux for 4 h. After the reaction was cooled, the reaction mixture was diluted with dichloromethane (120.0 mL), and then water was added dropwise at 0 °C to quench the reaction under vigorous stirring conditions. The solid which precipitated out was removed by filtration, and the organic layer obtained was dried over Na_2SO_4 . After the removal of the solvents in vacuo, the residue was purified to give SF47–SF55.

11b-Methyl-2,3,5,6,11,11b-hexahydro-1H-indolizino[8,7-b]indole (SF47): pale yellow oil (40.5 mg, yield 60%). 1H -NMR (400 MHz, $DMSO-d_6$) δ 1.67–1.54 (m, 1H), 1.80 (s, 3H), 2.04–1.93 (m, 1H), 2.20–2.08 (m, 1H), 2.94–2.85 (m, 1H), 3.07–2.96 (m, 1H), 3.30–3.22 (m, 2H), 3.56–3.47 (m, 3H), 7.05–6.99 (m, 1H), 7.15–7.09 (m, 1H), 7.35 (d, $J = 8.1$ Hz, 1H), 7.47 (d, $J = 7.8$ Hz, 1H), 11.28 (s, 1H); ^{13}C -NMR (125 MHz, $DMSO-d_6$) δ 136.3 (C, Ar), 125.7 (C, Ar), 121.8 (CH, Ar), 119.0 (CH, Ar), 118.3 (CH, Ar), 111.3 (CH, Ar), 104.5 (C, Ar), 48.9 (CH_2), 42.5 (CH_2), 36.4 (CH_2), 24.1 (CH_3), 21.0 (CH_2), 15.3 (CH_2); ESI-LRMS m/z : 227 [$M + H$] $^+$; ESI-HRMS m/z calcd for $M + H^+$ 227.1543, found: 227.1540.

13b-Methyl-7,8,13,13b-tetrahydro-5H-benzo[1,2]indolizino[8,7-b]indole (SF48a): pale yellow solid (52.3 mg, yield 64%), mp 204–206 °C. 1H -NMR (400 MHz, $CDCl_3$) δ 1.95 (s, 3H), 2.62–2.53 (m, 1H), 3.28–3.13 (m, 1H), 3.54–3.38 (m, 2H), 4.27–4.18 (m, 2H), 7.13–7.03 (m, 2H), 7.21–7.13 (m, 2H), 7.31–7.22 (m, 2H), 7.85–7.74 (m, 2H), 7.93 (s, 1H); ^{13}C -NMR (125 MHz, $DMSO-d_6$) δ 135.5 (C, Ar), 131.8 (C, Ar), 126.5 (CH, Ar), 126.4 (CH, Ar), 124.9 (C, Ar), 122.8 (CH, Ar), 122.4 (CH, Ar), 120.2 (CH, Ar), 119.0 (CH, Ar), 118.3 (CH, Ar), 110.8 (CH, Ar), 52.7 (CH_2), 41.0 (CH_2), 26.2 (CH_3), 17.1 (CH_2); ESI-LRMS m/z : 275 [$M + H$] $^+$; ESI-HRMS m/z calcd for $M + H^+$ 275.1543, found: 275.1541. The characterization data is in accordance with that reported in [43].

10-Methoxy-13b-methyl-7,8,13,13b-tetrahydro-5H-benzo[1,2]indolizino[8,7-b]indole (SF48b): pale yellow oil (59.2 mg, yield 65%). 1H -NMR (400 MHz, $CDCl_3$) δ 1.86 (s, 3H), 2.60 (ddd, $J = 15.8, 4.3, 1.4$ Hz, 1H), 3.13 (ddd, $J = 16.2, 11.1, 6.4$ Hz, 1H), 3.54–3.43 (m, 2H), 3.84 (s, 3H), 4.26–4.15 (m, 2H), 6.78 (dd, $J = 8.7, 2.5$ Hz, 1H), 6.93 (d, $J = 2.4$ Hz, 1H), 7.15 (d, $J = 8.7$ Hz, 1H), 7.25–7.18 (m, 2H), 7.33–7.27 (m, 1H), 7.45 (d, $J = 7.4$ Hz, 1H), 7.60 (s, 1H); ^{13}C -NMR (100 MHz, $CDCl_3$) δ 154.2 (C, Ar), 144.9 (C, Ar), 139.0 (C, Ar), 137.8 (C, Ar), 131.3 (C, Ar), 127.7 (CH, Ar), 127.7 (C, Ar), 127.4 (CH, Ar), 123.4 (CH, Ar), 121.1 (CH, Ar), 111.7 (CH, Ar), 111.7 (CH, Ar), 106.9 (C, Ar), 100.9 (CH, Ar), 65.0 (C), 56.1 (OCH_3), 53.2 (CH_2), 41.7 (CH_2), 26.0 (CH_3), 16.4 (CH_2); ESI-LRMS m/z : 305 [$M + H$] $^+$; ESI-HRMS m/z calcd for $M + H^+$ 305.1648, found: 305.1645. The characterization data is in accordance with that reported in [43].

14b-Methyl-5,6,8,9,14,14b-hexahydroindolo[2',3':3,4]pyrido[2,1-a]isoquinoline (SF49): pale yellow oil (60.2 mg, yield 70%). 1H -NMR (400 MHz, $CDCl_3$) δ 1.95 (s, 3H), 2.85–2.66 (m, 2H), 3.07–2.91 (m, 2H), 3.14–3.07 (m, 1H), 3.19–3.15 (m, 1H), 3.26 (ddd, $J = 13.8, 6.1, 2.6$ Hz, 1H), 3.76 (ddd, $J = 13.9, 10.0, 5.8$ Hz, 1H), 7.19–7.05 (m, 3H), 7.25–7.20 (m, 1H), 7.31–7.27 (m, 1H), 7.37–7.31 (m, 1H), 7.49 (d, $J = 7.6$ Hz, 1H), 7.65 (d, $J = 7.8$ Hz, 1H), 7.87 (s, 1H); ^{13}C -NMR (100 MHz, $CDCl_3$) δ 140.0 (C, Ar), 137.5 (C, Ar), 135.8 (C, Ar), 134.5 (C, Ar), 130.1 (CH, Ar), 127.7 (C, Ar), 126.8 (CH, Ar), 126.6 (CH, Ar), 126.0 (CH, Ar), 121.8 (CH, Ar), 119.6 (CH, Ar), 118.5 (CH, Ar), 111.0 (CH, Ar), 105.9 (C, Ar), 58.3 (C), 46.8 (CH_2), 45.5 (CH_2), 30.4 (CH_3), 28.8 (CH_2), 17.9 (CH_2); ESI-LRMS m/z : 289 [$M + H$] $^+$; ESI-HRMS m/z calcd for $M + H^+$ 289.1699, found: 289.1695. The characterization data is in accordance with that reported in [43].

11c-Methyl-2,3,5,6,7,11c-hexahydro-1H-indolizino[7,8-b]indole (SF50): pale yellow solid (62.2 mg, yield 92%), mp 249–250 °C. 1H -NMR (400 MHz, $DMSO-d_6$) δ 1.66–1.51 (m, 1H), 1.82 (s, 3H), 2.04–1.92 (m, 1H), 2.27–2.15 (m, 1H), 2.61–2.52 (m, 1H), 3.02–2.87 (m, 1H), 3.24–3.13 (m, 1H), 3.31–3.25 (m, 1H), 3.60–3.44 (m, 3H), 7.04–6.97 (m, 1H), 7.13–7.07 (m, 1H), 7.35 (d, $J = 8.0$ Hz, 1H), 7.51 (d, $J = 7.9$ Hz, 1H), 11.24 (s, 1H); ^{13}C -NMR (125 MHz, $DMSO-d_6$) δ 136.2 (C, Ar), 129.5 (C, Ar), 123.3 (C, Ar), 121.3 (CH,

Ar), 119.0 (CH, Ar), 118.0 (CH, Ar), 111.4 (CH, Ar), 48.7 (CH₂), 41.8 (CH₂), 36.1 (CH₂), 24.3 (CH₃), 21.2 (CH₂), 16.8 (CH₂); ESI-LRMS *m/z*: 227 [M + H]⁺; ESI-HRMS *m/z* calcd for M + H⁺ 227.1543, found: 227.1541.

14c-Methyl-5,6,8,9,10,14c-hexahydroindolo[3',2':3,4]pyrido[2,1-a]isoquinoline (SF51): pale yellow oil (63.5 mg, yield 73%). ¹H-NMR (600 MHz, CDCl₃) δ 2.21 (s, 3H), 2.82–2.75 (m, 1H), 2.97 (dd, *J* = 17.9, 6.5 Hz, 1H), 3.23–3.17 (m, 1H), 3.32–3.27 (m, 2H), 3.42–3.38 (m, 1H), 3.50–3.43 (m, 1H), 4.15–4.07 (m, 1H), 7.10–7.05 (m, 2H), 7.14–7.10 (m, 2H), 7.20–7.16 (m, 1H), 7.31 (d, *J* = 8.0 Hz, 1H), 7.65 (d, *J* = 7.9 Hz, 1H), 7.79 (d, *J* = 7.9 Hz, 1H), 9.64 (s, 1H); ¹³C-NMR (150 MHz, CDCl₃) δ 142.9 (C, Ar), 136.6 (C, Ar), 132.7 (C, Ar), 131.2 (C, Ar), 129.2 (CH, Ar), 128.1 (CH, Ar), 127.3 (C, Ar), 126.3 (2 × CH, Ar), 120.8 (CH, Ar), 120.7 (CH, Ar), 119.5 (CH, Ar), 115.3 (C, Ar), 111.2 (CH, Ar), 59.8 (C), 45.8 (CH₂), 45.3 (CH₂), 29.9 (CH₃), 23.6 (CH₂), 23.1 (CH₂); ESI-LRMS *m/z*: 289 [M + H]⁺; ESI-HRMS *m/z* calcd for M + H⁺ 289.1699, found: 289.1698.

15b-Methyl-6,8,9,15b-tetrahydro-5H-indolo[2',1':3,4]pyrazino[2,1-a]isoquinoline (SF52): pale yellow oil (34.3 mg, yield 40%). ¹H-NMR (600 MHz, CDCl₃) δ 1.94 (s, 3H), 2.92–2.83 (m, 1H), 3.07–2.99 (m, 1H), 3.17–3.09 (m, 1H), 3.40–3.32 (m, 1H), 3.55–3.47 (m, 1H), 3.63–3.56 (m, 1H), 4.08–4.01 (m, 1H), 4.15–4.10 (m, 1H), 6.55 (s, 1H), 7.15–7.10 (m, 2H), 7.20–7.15 (m, 3H), 7.27 (d, *J* = 8.0 Hz, 1H), 7.63–7.57 (m, 2H); ¹³C-NMR (150 MHz, CDCl₃) δ 140.9 (C, Ar), 139.8 (C, Ar), 136.7 (C, Ar), 132.8 (C, Ar), 129.5 (CH, Ar), 128.0 (C, Ar), 127.8 (CH, Ar), 126.6 (CH, Ar), 126.1 (CH, Ar), 121.2 (CH, Ar), 120.3 (CH, Ar), 120.1 (CH, Ar), 109.1 (CH, Ar), 100.6 (CH, Ar), 59.2 (C), 45.7 (CH₂), 45.6 (CH₂), 40.4 (CH₂), 31.5 (CH₃), 25.3 (CH₂); ESI-LRMS *m/z*: 289 [M + H]⁺; ESI-HRMS *m/z* calcd for M + H⁺ 289.1699, found: 289.1696.

11b-Methyl-4,5,7,11b-tetrahydro-3H-pyrrolo[3',2':3,4]pyrido[2,1-a]isoindole (SF53): pale yellow oil (57.2 mg, yield 85%). ¹H-NMR (600 MHz, CDCl₃) δ 1.78 (s, 3H), 3.07–2.97 (m, 1H), 3.49–3.36 (m, 2H), 3.72–3.65 (m, 1H), 4.18–4.11 (m, 1H), 4.28–4.20 (m, 1H), 6.08–6.04 (m, 1H), 6.62–6.58 (m, 1H), 7.19–7.14 (m, 2H), 7.29–7.23 (m, 1H), 7.45–7.40 (m, 1H), 7.83 (s, 1H); ¹³C-NMR (150 MHz, CDCl₃) δ 148.1 (C, Ar), 137.8 (C, Ar), 127.2 (CH, Ar), 126.8 (CH, Ar), 122.9 (C, Ar), 122.7 (CH, Ar), 121.9 (1CH + 1C, Ar), 116.6 (CH, Ar), 105.2 (CH, Ar), 65.8 (C), 53.5 (CH₂), 42.1 (CH₂), 28.2 (CH₃), 17.2 (CH₂); ESI-LRMS *m/z*: 225 [M + H]⁺; ESI-HRMS *m/z* calcd for M + H⁺ 225.1386, found: 225.1385.

11b-Methyl-4,5,7,11b-tetrahydrothieno[3',2':3,4]pyrido[2,1-a]isoindole (SF54): pale yellow solid (57.9 mg, yield 80%), mp 73–74 °C. ¹H-NMR (600 MHz, CDCl₃) δ 1.76 (s, 3H), 2.60 (ddd, *J* = 16.5, 4.4, 1.5 Hz, 1H), 3.22–3.13 (m, 1H), 3.49–3.38 (m, 2H), 4.20–4.12 (m, 2H), 6.94 (d, *J* = 5.2 Hz, 1H), 7.00 (dd, *J* = 5.3, 0.7 Hz, 1H), 7.21–7.17 (m, 2H), 7.28–7.25 (m, 1H), 7.45 (d, *J* = 7.6 Hz, 1H); ¹³C-NMR (150 MHz, CDCl₃) δ 146.7 (C, Ar), 139.5 (C, Ar), 138.6 (C, Ar), 132.4 (C, Ar), 127.1 (2 × CH, Ar), 125.6 (CH, Ar), 122.8 (CH, Ar), 122.3 (CH, Ar), 122.1 (CH, Ar), 67.0 (C, Ar), 53.6 (CH₂), 42.1 (CH₂), 27.9 (CH₃), 19.2 (CH₂); ESI-LRMS *m/z*: 242 [M + H]⁺; ESI-HRMS *m/z* calcd for M + H⁺ 242.0998, found: 242.0997.

11b-Methyl-4,5,7,11b-tetrahydrothieno[2',3':3,4]pyrido[2,1-a]isoindole (SF55): yellow oil (68.6 mg, yield 95%). ¹H-NMR (600 MHz, CDCl₃) δ 1.85 (s, 3H), 2.47 (ddd, *J* = 16.4, 4.5, 1.4 Hz, 1H), 3.07–2.97 (m, 1H), 3.45–3.30 (m, 2H), 4.22–4.12 (m, 2H), 6.69 (d, *J* = 5.1 Hz, 1H), 7.11 (d, *J* = 5.0 Hz, 1H), 7.18–7.16 (m, 1H), 7.21–7.18 (m, 1H), 7.30–7.26 (m, 1H), 7.46 (d, *J* = 7.6 Hz, 1H); ¹³C-NMR (150 MHz, CDCl₃) δ 147.2 (C, Ar), 142.4 (C, Ar), 138.4 (C, Ar), 132.5 (C, Ar), 127.3 (2 × CH, Ar), 126.9 (CH, Ar), 123.1 (CH, Ar), 122.8 (CH, Ar), 122.1 (CH, Ar), 67.0 (C), 53.7 (CH₂), 41.8 (CH₂), 29.8 (CH₃), 20.2 (CH₂); ESI-LRMS *m/z*: 242 [M + H]⁺; ESI-HRMS *m/z* calcd for M + H⁺ 242.0998, found: 242.0997.

4. Conclusions

In conclusion, a green and general tandem reaction between alkynoic acids and amine nucleophiles through gold catalysis in water has been developed. This process proceeds with high efficiency leading to the formation of two rings and three new bonds in a single operation. This approach features low catalyst loading, good to excellent yields, high efficiency in bond formation, high step economy, excellent selectivity, great functional group tolerance, and extraordinarily

broad substrate scope, and has been successfully employed to construct a high-quality library of indole/thiophene/pyrrole/pyridine/naphthalene/benzene-fused *N*-heterocycles. In addition, five antimicrobial compounds were discovered from the library, suggesting the value of our strategy to identify APIs. This is the first example of the generation of pDOS compound library encompassing skeletal diversity, molecular complexity, and drug-like properties from readily available materials through gold catalysis in water. We anticipate that these valuable *N*-heterocycles will find more pharmaceutical applications after our further investigations.

Supplementary Materials: The following are available online. Table S1: Survey of the solvents on the yield of product **SF1a**, Figures S1–S12: NMR (¹H-NMR, ¹³C-NMR, HSQC, HMBC, and ¹H-¹H COSY) and ESI(+)-MS spectrum of **SF5a**, [D]_n-**SF5a**, **SF5b**, [D]_n-**SF5b**, **SF1a**, and [D]_n-**SF1a**. Figure S13: preliminary screening of antibacterial activities of compounds at 100 µg/mL. Figures S14–S19: time-kill results of **SF9d**, **SF29b**, **SF33**, **SF36**, and **SF41** against *S. aureus* strain. Figures S20–S24: CFU results of compounds **SF9d**, **SF29b**, **SF33**, **SF36** and **SF41**; copies of ¹H and ¹³C-NMR spectra of new compounds.

Author Contributions: Conceptualization, H.L. and F.Z.; Methodology, X.J. and X.L.; Formal Analysis, J.Y., J.L., and F.Z.; Investigation, X.J., P.L., and J.L.; Resources, Y.C. and X.L.; Writing—Original Draft Preparation, J.L. and F.Z.; Writing—Review and Editing, F.Z., J.W., and H.L.; Visualization, F.Z.; Supervision, H.L. and F.Z.; Project Administration, F.Z.; Funding Acquisition, J.L., H.L., and F.Z.

Funding: This research was funded by the National Natural Science Foundation of China (grants 21602022, 81620108027, and 21632008), the Major Project of Chinese National Programs for Fundamental Research and Development (grant 2015CB910304), Sichuan Science and Technology Program (grants 2018JY0345 and 2018HH007), and Chengdu Municipal Government Program of Science and Technology (grant 2016-XT00-00023-GX). The APC was funded by Chengdu University New Faculty Start-up Funding (grant 2081915037).

Acknowledgments: F.Z. gratefully acknowledges the support from the 1000 Talents Program of Sichuan Province and Chengdu Talents Program.

Conflicts of Interest: The authors declare no conflict of interest.

References

1. Yarmush, M.L.; Jayaraman, A. Advances in proteomic technologies. *Annu. Rev. Biomed. Eng.* **2002**, *4*, 349–373. [[CrossRef](#)] [[PubMed](#)]
2. Aebersold, R.; Cravatt, B.F. Proteomics—advances, applications and the challenges that remain. *Trends Biotechnol.* **2002**, *20*, S1–S2. [[CrossRef](#)]
3. Yee, A.; Pardee, K.; Christendat, D.; Savchenko, A.; Edwards, A.M.; Arrowsmith, C.H. Structural proteomics: Toward high-throughput structural biology as a tool in functional genomics. *Acc. Chem. Res.* **2003**, *36*, 183–189. [[CrossRef](#)] [[PubMed](#)]
4. Cottingham, K. Government & society: New cancer center will focus on proteomics and genomics. *J. Proteome Res.* **2007**, *6*, 3369.
5. Yates, J.R.; Osterman, A.L. Introduction: Advances in genomics and proteomics. *Chem. Rev.* **2007**, *107*, 3363–3366.
6. Bleicher, K.H.; Böhm, H.J.; Müller, K.; Alanine, A.I. A guide to drug discovery: Hit and lead generation: Beyond high-throughput screening. *Nat. Rev. Drug Discov.* **2003**, *2*, 369–378. [[CrossRef](#)] [[PubMed](#)]
7. Drewry, D.H.; Macarron, R. Enhancements of screening collections to address areas of unmet medical need: An industry perspective. *Curr. Opin. Chem. Biol.* **2010**, *14*, 289–298. [[CrossRef](#)] [[PubMed](#)]
8. Dandapani, S.; Marcaurelle, L.A. Grand challenge commentary: Accessing new chemical space for ‘undruggable’ targets. *Nat. Chem. Biol.* **2010**, *6*, 861–863. [[CrossRef](#)] [[PubMed](#)]
9. Sauer, W.H.B.; Schwarz, M.K. Molecular shape diversity of combinatorial libraries: A prerequisite for broad bioactivity. *J. Chem. Inf. Comput. Sci.* **2003**, *43*, 987–1003. [[CrossRef](#)] [[PubMed](#)]
10. Haggarty, S.J. The principle of complementarity: Chemical versus biological space. *Curr. Opin. Chem. Biol.* **2005**, *9*, 296–303. [[CrossRef](#)] [[PubMed](#)]
11. Quinn, R.J.; Carroll, A.R.; Pham, N.B.; Baron, P.; Palframan, M.E.; Suraweera, L.; Pierens, G.K.; Muresan, S. Developing a drug-like natural product library. *J. Nat. Prod.* **2008**, *71*, 464–468. [[CrossRef](#)] [[PubMed](#)]
12. Camp, D.; Davis, R.A.; Campitelli, M.; Ebdon, J.; Quinn, R.J. Drug-like properties: Guiding principles for the design of natural product libraries. *J. Nat. Prod.* **2012**, *75*, 72–81. [[CrossRef](#)] [[PubMed](#)]

13. Dandapani, S.; Rosse, G.; Southall, N.; Salvino, J.M.; Thomas, C.J. Selecting, acquiring, and using small molecule libraries for high-throughput screening. *Curr. Protoc. Chem. Biol.* **2012**, *4*, 177–191. [[PubMed](#)]
14. Rzuczek, S.G.; Southern, M.R.; Disney, M.D. Studying a drug-like, RNA-focused small molecule library identifies compounds that inhibit RNA toxicity in myotonic dystrophy. *ACS Chem. Biol.* **2015**, *10*, 2706–2715. [[CrossRef](#)] [[PubMed](#)]
15. Evans, B.E.; Rittle, K.E.; Bock, M.G.; DiPardo, R.M.; Freidinger, R.M.; Whitter, W.L.; Lundell, G.F.; Veber, D.F.; Anderson, P.S.; Chang, R.S.L.; et al. Methods for drug discovery: Development of potent, selective, orally effective cholecystokinin antagonists. *J. Med. Chem.* **1988**, *31*, 2235–2246. [[CrossRef](#)] [[PubMed](#)]
16. Horton, D.A.; Bourne, G.T.; Smythe, M.L. The combinatorial synthesis of bicyclic privileged structures or privileged substructures. *Chem. Rev.* **2003**, *103*, 893–930. [[CrossRef](#)] [[PubMed](#)]
17. DeSimone, R.W.; Currie, K.S.; Mitchell, S.A.; Darrow, J.W.; Pippin, D.A. Privileged structures: Applications in drug discovery. *Comb. Chem. High Throughput Screen.* **2004**, *7*, 473–494. [[CrossRef](#)] [[PubMed](#)]
18. Welsch, M.E.; Snyder, S.A.; Stockwell, B.R. Privileged scaffolds for library design and drug discovery. *Curr. Opin. Chem. Biol.* **2010**, *14*, 347–361. [[CrossRef](#)] [[PubMed](#)]
19. González, J.F.; Ortín, I.; de la Cuesta, E.; Menéndez, J.C. Privileged scaffolds in synthesis: 2,5-piperazinediones as templates for the preparation of structurally diverse heterocycles. *Chem. Soc. Rev.* **2012**, *41*, 6902–6915. [[CrossRef](#)] [[PubMed](#)]
20. Schreiber, S.L. Target-oriented and diversity-oriented organic synthesis in drug discovery. *Science* **2000**, *287*, 1964–1969. [[CrossRef](#)] [[PubMed](#)]
21. Reayi, A.; Arya, P. Natural product-like chemical space: Search for chemical dissectors of macromolecular interactions. *Curr. Opin. Chem. Biol.* **2005**, *9*, 240–247. [[CrossRef](#)] [[PubMed](#)]
22. Spandl, R.J.; Bender, A.; Spring, D.R. Diversity-oriented synthesis; a spectrum of approaches and results. *Org. Biomol. Chem.* **2008**, *6*, 1149–1158. [[CrossRef](#)] [[PubMed](#)]
23. Oh, S.; Park, S.B. A design strategy for drug-like polyheterocycles with privileged substructures for discovery of specific small-molecule modulators. *Chem. Commun.* **2011**, *47*, 12754–12761. [[CrossRef](#)] [[PubMed](#)]
24. Liu, H. Construction of biologically potential library by diversity-oriented synthesis. *Org. Chem. Curr. Res.* **2013**, *2*, 1000e123. [[CrossRef](#)]
25. Kim, H.; Tung, T.T.; Park, S.B. Privileged substructure-based diversity-oriented synthesis pathway for diverse pyrimidine-embedded polyheterocycles. *Org. Lett.* **2013**, *15*, 5814–5817. [[CrossRef](#)] [[PubMed](#)]
26. Kim, J.; Jung, J.; Koo, J.; Cho, W.; Lee, W.S.; Kim, C.; Park, W.; Park, S.B. Diversity-oriented synthetic strategy for developing a chemical modulator of protein–protein interaction. *Nat. Commun.* **2016**, *7*, 13196. [[CrossRef](#)] [[PubMed](#)]
27. Zhang, X.; Ye, D.; Sun, H.; Guo, D.; Wang, J.; Huang, H.; Zhang, X.; Jiang, H.; Liu, H. Microwave-assisted synthesis of quinazolinone derivatives by efficient and rapid iron-catalyzed cyclization in water. *Green Chem.* **2009**, *11*, 1881–1888. [[CrossRef](#)]
28. Ye, D.; Wang, J.; Zhang, X.; Zhou, Y.; Ding, X.; Feng, E.; Sun, H.; Liu, G.; Jiang, H.; Liu, H. Gold-catalyzed intramolecular hydroamination of terminal alkynes in aqueous media: Efficient and regioselective synthesis of indole-1-carboxamides. *Green Chem.* **2009**, *11*, 1201–1208. [[CrossRef](#)]
29. Zhou, Y.; Zhai, Y.; Li, J.; Ye, D.; Jiang, H.; Liu, H. Metal-free tandem reaction in water: An efficient and regioselective synthesis of 3-hydroxyisoindolin-1-ones. *Green Chem.* **2010**, *12*, 1397–1404. [[CrossRef](#)]
30. Zhang, X.; Zhou, Y.; Wang, H.; Guo, D.; Ye, D.; Xu, Y.; Jiang, H.; Liu, H. Silver-catalyzed intramolecular hydroamination of alkynes in aqueous media: Efficient and regioselective synthesis for fused benzimidazoles. *Green Chem.* **2011**, *13*, 397–405. [[CrossRef](#)]
31. Xu, S.; Zhou, Y.; Xu, J.; Jiang, H.; Liu, H. Gold-catalyzed Michael addition/intramolecular annulation cascade: An effective pathway for the chemoselective- and regioselective synthesis of tetracyclic indole derivatives in water. *Green Chem.* **2013**, *15*, 718–726. [[CrossRef](#)]
32. Yang, T.; Campbell, L.; Dixon, D.J. A Au(I)-catalyzed N-acyl iminium ion cyclization cascade. *J. Am. Chem. Soc.* **2007**, *129*, 12070–12071. [[CrossRef](#)] [[PubMed](#)]
33. Muratore, M.E.; Holloway, C.A.; Pilling, A.W.; Storer, R.I.; Trevitt, G.; Dixon, D.J. Enantioselective Brønsted acid-catalyzed N-acyliminium cyclization cascades. *J. Am. Chem. Soc.* **2009**, *131*, 10796–10797. [[CrossRef](#)] [[PubMed](#)]

34. Patil, N.T.; Mutyala, A.K.; Lakshmi, P.G.V.V.; Gajula, B.; Sridhar, B.; Pottireddygar, G.R.; Rao, T.P. Au(I)-catalyzed cascade reaction involving formal double hydroamination of alkynes bearing tethered carboxylic groups: An easy access to fused dihydrobenzimidazoles and tetrahydroquinazolines. *J. Org. Chem.* **2010**, *75*, 5963–5975. [[CrossRef](#)] [[PubMed](#)]
35. Feng, E.; Zhou, Y.; Zhang, D.; Zhang, L.; Sun, H.; Jiang, H.; Liu, H. Gold(I)-catalyzed tandem transformation: A simple approach for the synthesis of pyrrolo/pyrido[2,1-*a*][1,3]benzoxazinones and pyrrolo/pyrido[2,1-*a*]quinazolinones. *J. Org. Chem.* **2010**, *75*, 3274–3282. [[CrossRef](#)] [[PubMed](#)]
36. Zhou, Y.; Zhai, Y.; Ji, X.; Liu, G.; Feng, E.; Ye, D.; Zhao, L.; Jiang, H.; Liu, H. Gold(I)-catalyzed one-pot tandem coupling/cyclization: An efficient synthesis of pyrrolo-/pyrido[2,1-*b*]benzo[*d*][1,3]oxazin-1-ones. *Adv. Synth. Catal.* **2010**, *352*, 373–378. [[CrossRef](#)]
37. Zhou, Y.; Li, J.; Ji, X.; Zhou, W.; Zhang, X.; Qian, W.; Jiang, H.; Liu, H. Silver- and gold-mediated domino transformation: A strategy for synthesizing benzo[*e*]indolo[1,2-*a*]pyrrolo/pyrido[2,1-*c*][1,4]diazepine-3,9-diones. *J. Org. Chem.* **2011**, *76*, 1239–1249. [[CrossRef](#)] [[PubMed](#)]
38. Patil, N.T.; Lakshmi, P.G.V.V.; Sridhar, B.; Patra, S.; Bhadra, M.P.; Patra, C.R. New linearly and angularly fused quinazolinones: Synthesis through gold(I)-catalyzed cascade reactions and anticancer activities. *Eur. J. Org. Chem.* **2012**, 1790–1799. [[CrossRef](#)]
39. Li, Z.; Li, J.; Yang, N.; Chen, Y.; Zhou, Y.; Ji, X.; Zhang, L.; Wang, J.; Xie, X.; Liu, H. Gold(I)-catalyzed cascade approach for the synthesis of tryptamine-based polycyclic privileged scaffolds as α_1 -adrenergic receptor antagonists. *J. Org. Chem.* **2013**, *78*, 10802–10811. [[CrossRef](#)] [[PubMed](#)]
40. Ji, X.; Zhou, Y.; Wang, J.; Zhao, L.; Jiang, H.; Liu, H. Au(I)/Ag(I)-catalyzed cascade approach for the synthesis of benzo[4,5]imidazo[1,2-*c*]pyrrolo[1,2-*a*]quinazolinones. *J. Org. Chem.* **2013**, *78*, 4312–4318. [[CrossRef](#)] [[PubMed](#)]
41. Patil, N.T.; Shinde, V.S.; Sridhar, B. Relay catalytic branching cascade: A technique to access diverse molecular scaffolds. *Angew. Chem. Int. Ed.* **2013**, *52*, 2251–2255. [[CrossRef](#)] [[PubMed](#)]
42. Naidu, S.; Reddy, S.R. Copper-catalyzed tandem reaction in ionic liquid: An efficient reusable catalyst and solvent media for the synthesis of fused poly hetero cyclic compounds. *RSC Adv.* **2016**, *6*, 62742–62746. [[CrossRef](#)]
43. Qiao, J.; Jia, X.; Li, P.; Liu, X.; Zhao, J.; Zhou, Y.; Wang, J.; Liu, H.; Zhao, F. Gold-catalyzed rapid construction of nitrogen-containing heterocyclic compound library with scaffold diversity and molecular complexity. *Adv. Synth. Catal.* **2019**, 361. [[CrossRef](#)]
44. Zhou, Y.; Ji, X.; Liu, G.; Zhang, D.; Zhao, L.; Jiang, H.; Liu, H. Gold(I)-catalyzed cascade for synthesis of pyrrolo[1,2-*a*:2',1'-*c*]-/Pyrido[2,1-*c*]pyrrolo[1,2-*a*]quinoxalinones. *Adv. Synth. Catal.* **2010**, *352*, 1711–1717. [[CrossRef](#)]
45. Feng, E.; Zhou, Y.; Zhao, F.; Chen, X.; Zhang, L.; Jiang, H.; Liu, H. Gold-catalyzed tandem reaction in water: An efficient and convenient synthesis of fused polycyclic indoles. *Green Chem.* **2012**, *14*, 1888–1895. [[CrossRef](#)]
46. Aplander, K.; Hidestøl, O.; Katebzadeh, K.; Lindström, U.M. A green and facile route to γ - and δ -lactones via efficient Pinner-cyclization of hydroxynitriles in water. *Green Chem.* **2006**, *8*, 22–24. [[CrossRef](#)]
47. Li, C.J.; Chen, L. Organic chemistry in water. *Chem. Soc. Rev.* **2006**, *35*, 68–82. [[CrossRef](#)] [[PubMed](#)]
48. Chanda, A.; Fokin, V.V. Organic synthesis “on water”. *Chem. Rev.* **2009**, *109*, 725–748. [[CrossRef](#)] [[PubMed](#)]
49. Kumaravel, K.; Vasuki, G. Multi-component reactions in water. *Curr. Org. Chem.* **2009**, *13*, 1820–1841. [[CrossRef](#)]
50. Gupta, M.; Paul, S.; Gupta, R. General aspects of 12 basic principles of green chemistry with applications. *Curr. Sci.* **2010**, *99*, 1341–1360.
51. Butler, R.N.; Coyne, A.G. Water: Nature’s reaction enforcer—Comparative effects for organic synthesis “in-water” and “on-water”. *Chem. Rev.* **2010**, *110*, 6302–6337. [[CrossRef](#)] [[PubMed](#)]
52. Hashmi, A.S.K. Gold-catalyzed organic reactions. *Chem. Rev.* **2007**, *107*, 3180–3211. [[CrossRef](#)] [[PubMed](#)]
53. Corma, A.; Leyva-Pérez, A.; Sabater, M.J. Gold-catalyzed carbon–heteroatom bond-forming reactions. *Chem. Rev.* **2011**, *111*, 1657–1712. [[CrossRef](#)] [[PubMed](#)]
54. Huang, H.; Zhou, Y.; Liu, H. Recent advances in the gold-catalyzed additions to C–C multiple bonds. *Beilstein J. Org. Chem.* **2011**, *7*, 897–936. [[CrossRef](#)] [[PubMed](#)]
55. Krause, N.; Winter, C. Gold-catalyzed nucleophilic cyclization of functionalized allenes: A powerful access to carbo- and heterocycles. *Chem. Rev.* **2011**, *111*, 1994–2009. [[CrossRef](#)] [[PubMed](#)]

56. Dorel, R.; Echavarren, A.M. Gold(I)-catalyzed activation of alkynes for the construction of molecular complexity. *Chem. Rev.* **2015**, *115*, 9028–9072. [[CrossRef](#)] [[PubMed](#)]
57. Gao, F.; Zhou, Y.; Liu, H. Recent advances in the synthesis of heterocycles via gold-catalyzed cascade reactions: A review. *Curr. Org. Chem.* **2017**, *21*, 1530–1566. [[CrossRef](#)]
58. Dalpozzo, R. Strategies for the asymmetric functionalization of indoles: An update. *Chem. Soc. Rev.* **2015**, *44*, 742–778. [[CrossRef](#)] [[PubMed](#)]
59. Lindner, A.; Claassen, V.; Hendriksen, T.W.J.; Kralt, T. Reserpine analogs; phenethylamine derivatives¹. *J. Med. Chem.* **1963**, *6*, 97–101. [[CrossRef](#)] [[PubMed](#)]
60. Daugan, A.; Grondin, P.; Ruault, C.; de Gouville, A.C.L.M.; Coste, H.; Kirilovsky, J.; Hyafil, F.; Labaudinière, R. The discovery of Tadalafil: A novel and highly selective PDE5 inhibitor. 1: 5,6,11,11a-tetrahydro-1H-imidazo[1',5':1,6]pyrido[3,4-b]indole-1,3(2H)-dione analogues. *J. Med. Chem.* **2003**, *46*, 4525–4532. [[CrossRef](#)] [[PubMed](#)]
61. Daugan, A.; Grondin, P.; Ruault, C.; de Gouville, A.C.L.M.; Coste, H.; Linget, J.M.; Kirilovsky, J.; Hyafil, F.; Labaudinière, R. The discovery of Tadalafil: A novel and highly selective PDE5 inhibitor. 2: 2,3,6,7,12,12a-hexahydropyrazino[1',2':1,6]pyrido[3,4-b]indole-1,4-dione analogues. *J. Med. Chem.* **2003**, *46*, 4533–4542. [[CrossRef](#)] [[PubMed](#)]
62. Kochanowska-Karamyan, A.J.; Hamann, M.T. Marine indole alkaloids: Potential new drug leads for the control of depression and anxiety. *Chem. Rev.* **2010**, *110*, 4489–4497. [[CrossRef](#)] [[PubMed](#)]
63. Silvestri, R. New prospects for vinblastine analogues as anticancer agents. *J. Med. Chem.* **2013**, *56*, 625–627. [[CrossRef](#)] [[PubMed](#)]
64. Sun, H.; Zhu, L.; Yang, H.; Qian, W.; Guo, L.; Zhou, S.; Gao, B.; Li, Z.; Zhou, Y.; Jiang, H.; et al. Asymmetric total synthesis and identification of tetrahydroprotoberberine derivatives as new antipsychotic agents possessing a dopamine D₁, D₂ and serotonin 5-HT_{1A} multi-action profile. *Bioorg. Med. Chem.* **2013**, *21*, 856–868. [[CrossRef](#)] [[PubMed](#)]
65. Guo, D.; Li, J.; Lin, H.; Zhou, Y.; Chen, Y.; Zhao, F.; Sun, H.; Zhang, D.; Li, H.; Shoichet, B.K.; et al. Design, synthesis, and biological evaluation of novel tetrahydroprotoberberine derivatives (THPBs) as selective α_{1A} -adrenoceptor antagonists. *J. Med. Chem.* **2016**, *59*, 9489–9502. [[CrossRef](#)] [[PubMed](#)]
66. Stempel, E.; Gaich, T. Cyclohepta[b]indoles: A privileged structure motif in natural products and drug design. *Acc. Chem. Res.* **2016**, *49*, 2390–2402. [[CrossRef](#)] [[PubMed](#)]
67. Homer, J.A.; Sperry, J. Mushroom-derived indole alkaloids. *J. Nat. Prod.* **2017**, *80*, 2178–2187. [[CrossRef](#)] [[PubMed](#)]
68. Klas, K.R.; Kato, H.; Frisvad, J.C.; Yu, F.; Newmister, S.A.; Fraley, A.E.; Sherman, D.H.; Tsukamoto, S.; Williams, R.M. Structural and stereochemical diversity in prenylated indole alkaloids containing the bicyclo[2.2.2]diazoctane ring system from marine and terrestrial fungi. *Nat. Prod. Rep.* **2018**, *35*, 532–558. [[CrossRef](#)] [[PubMed](#)]
69. Sun, H.; Huang, H.; Zhang, D.; Feng, E.; Qian, W.; Zhang, L.; Chen, K.; Liu, H. Synthesis of 4-aryl-2(5H)-furanones by gold(I)-catalyzed intramolecular annulation. *Adv. Synth. Catal.* **2011**, *353*, 1413–1419. [[CrossRef](#)]

Sample Availability: Samples of the compounds SF1–SF43, SF47–SF55 are available from the authors.



© 2019 by the authors. Licensee MDPI, Basel, Switzerland. This article is an open access article distributed under the terms and conditions of the Creative Commons Attribution (CC BY) license (<http://creativecommons.org/licenses/by/4.0/>).